Variability of Sea Ice Extent Along The East Coast of Greenland

2013-06-01

Author: Isabella Grönfeldt
Bachelor thesis, 15 hp
Lund University

Supervisors: Martin Nissen, Centre for Ocean and Ice, DMI
Elna Heimdal Nilsson, Combustion Physics, LU

LUND UNIVERSITY

-Front page image: personal photograph by Martin Nissen
displaying sea ice outside of Greenland.-

Abstract

There has been a decrease in sea ice extent and volume in the polar regions during the past decades; this study focuses on the Northern Hemisphere. The variability of the sea ice extent along the east coast of Greenland is examined and the area is divided into three regional zones to be able to study variations in the correlation strength along the coast. The ice extent along the east coast is achieved from highly accurate, manually produced ice charts from the Danish Meteorology Institute (DMI). The data of the ice extent along the east coast of Greenland is compared to SSM/I data of the ice extent of the entire Northern Hemisphere, achieved from passive microwave sensors for the years 2005-2012. The annual maximum and minimum sea ice extent of the different regions are compared. It was expected to see a negative correlation between the extent in the Northern Hemisphere and along the east coast of Greenland but the results showed a clear non-correlation, with slightly higher R-squared values for the annual minimum period than for the maximum.

The ice extent is mainly dominated by the ice drift, which in turn is controlled by the wind which follows the isobars of the surface pressure systems. It is therefore expected that the sea ice extent along the east coast of Greenland is highly correlated to the pressure difference across the Fram Strait. In this study a linear dependence between the sea ice extent along the east coast of Greenland and the pressure difference across the Fram Strait is sought for the years 2000-2012. The pressure difference is achieved using a new method; by taking the pressure difference between two weather stations on either side of the Fram Strait it is possible to get an approximate strength and direction of the wind in the middle of the strait, and thereby on the dominating force of direction of the ice. The results of the comparisons between the ice extent along the east coast of Greenland and the pressure difference show a correlation, especially for the annual minimum extent with R-squared values around 0,3. It is concluded that the variability of the sea ice extent is not solely predicted by the pressure difference, and that more parameters must be accounted for such as the surface air temperature.

Table of Contents

1. Introduction

1.1. Background

There has been a decrease in sea ice extent (see figure 1.1a), as well as volume, in the polar regions during the past decades; this study focuses particularly on the Northern Hemisphere. The biggest rate of change in the ice extent on the Northern Hemisphere can be observed during the summer months around the annual minimum in September. The decrease is correlated with rising surface air temperature, resulting in longer sea ice melting periods and more open water areas [1]. This has resulted in a growing interest in sea ice observations and the Arctic sea ice is monitored on a daily basis. There are several different ways of observing the sea ice properties: in situ observations from ships, airplanes and weather stations, movement of drift buoys and satellite remote sensing. The sea ice data are processed, analysed and displayed in a number of different ways [1].

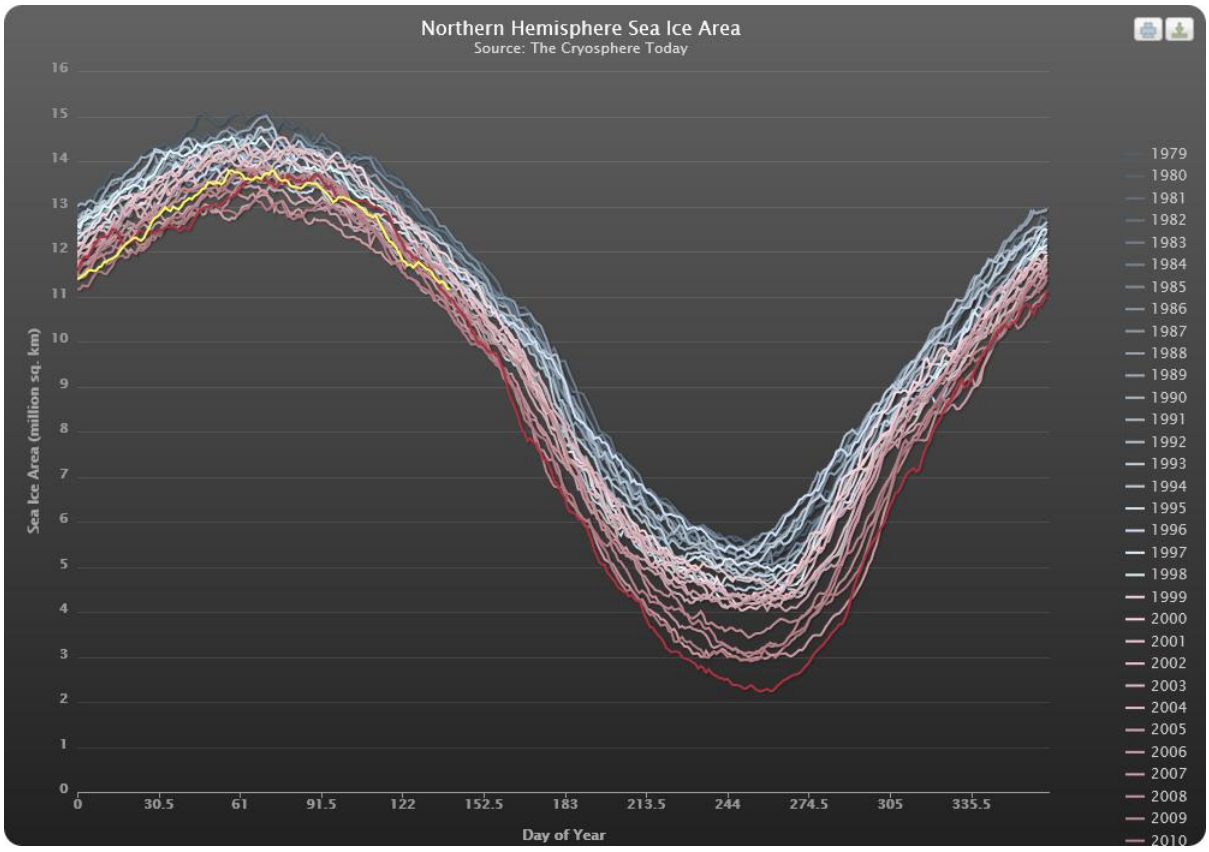

Figure 1.1a. Sea ice extent in the Northern Hemisphere has decreased during the previous decades. The graph shows the daily sea ice extent from SSM/I data, 1979-present. Note that the colour bar only displays the years 1979-2010 [2].

Many previous studies have been done on the variability of the sea ice, particularly in the central Arctic area and in the north-eastern part of Greenland [3, 4, 5, 6]. The Arctic Ocean holds the largest sea ice area in the Northern Hemisphere and most of its multiyear ice, see figure 1.1b. This ice is transported around in the ocean due to the dominant anticyclonic gyre and it may circle the Arctic for years before getting carried away by other currents. The second most dominant current in the Arctic is the Transpolar Drift Stream, it is the major transporter of ice out of the Arctic [7]. The current has a cross basin direction and pushes the

ice out through the Fram Strait, northeast of Greenland, making it a key area to study for sea ice drift and transport.

Even though the ice always seems to be pushed southward along the coast of Greenland, at a more or less high drift speed, it may take some time for the ice that passes through the Fram Strait to reach the south tip of Greenland. It is believed that a low extent of sea ice in the Arctic along with a strong southward wind, and thereby a strong Transpolar Drift Stream across the Arctic, leads to an accelerating sea ice drift out of the strait [8, 9]. It is clear that the ice extent is mainly determined by the ice drift, and a significant high velocity of the ice drift is found in Fram Strait [10]. This makes the area northeast of Greenland highly interesting for studies related to sea ice extent as well as drift. The ice drift is strongly correlated to the wind patterns and the wind is known to follow the isobars of atmospheric pressure systems. Thus there is expected to be a correlation between the ice extent along the east coast of Greenland and the pressure situation in the Fram Strait.

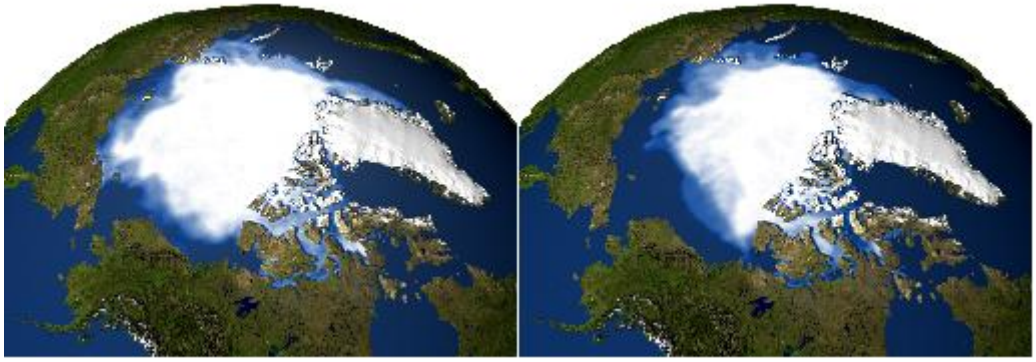

Figure 1.1b. The Arctic Ocean contains the largest area of sea ice in the Northern Hemisphere. To the left the annual minimum sea ice extent averaged between 1979-1981 and to the right between 2003-2005 [3].

Many studies have tried to find a correlation between the big atmospheric pressure systems and the sea ice drift as well as its extent in the Arctic region, like the North Atlantic (NAO) and Arctic Oscillations (AO) [10, 11, 12]. During limited periods of time a somewhat strong connection has been found, predominantly during the winter months and for a positive oscillation phase, but the results are not consistent [12]. So far there are no results that can prove a lasting connection between the atmospheric oscillations and the sea ice extent. However, the oscillations may explain the ice drift and thereby the ice extent for some specific occasions.

1.2. Purpose, method and expectations of the present study

In this study the variability of the sea ice extent along the east coast of Greenland is analysed during the period 2000-2012, by the use of data from in situ observations and satellite remote sensing, both direct images and manually created ice charts. The ice extent along the east coast of Greenland is compared to the extent in the entire Northern Hemisphere and to the pressure difference across the Fram Strait.

The focus is on the area along the east coast of Greenland, starting at the top of the Fram Strait and stretching down and just around the southern tip of Greenland. This area was chosen due to the strong ice drift in the area and its correlation with the ice extent. This study is special in the way that it compares two different sets of data, the continuous passive

microwave data for the entire Northern Hemisphere and the highly accurate sea ice charts over the east coast of Greenland both of which distributed by the Danish Meteorology Institute (DMI). The area of interest, i.e. the east coast of Greenland, is divided into three smaller zones to study the matter in a more small scale manner, which to the best knowledge of the author never has been done before.

This study compares the ice extent along the entire east coast of Greenland and the extent within three regional zones along the coast (see figure 1.2a), with the variability of the whole Northern Hemisphere, during the previous seven years (2005-2012). It examines the possibility of a correlation in the variability of the ice extents and what such a correlation/non-correlation may depend on. It is believed that if there is a correlation between the ice extent in the different regions it may be a negative one. The notion of a negative correlation is based on the fact that a decreased ice extent in the Arctic Ocean leads to increased mobility and a possible increase of ice efflux through the Fram Strait, resulting in an increased sea ice extent along the east coast of Greenland.

Figure 1.2a. Polygon image of the chosen region along the east coast of Greenland divided into the three smaller areas. The first and northernmost region (purple) is characterized by calm weather conditions and a shallow sea, the second and central region (green) by relative fast ice drift and deep waters while the third and southern region (red) is characterized by rough weather conditions and passing low pressure systems.

Furthermore in this study a comparison is made, for the period 2000-2012, between the ice extent along the east coast of Greenland and the pressure difference between the two sides of Fram Strait, i.e. the weather stations Henrik Krøyer Holme (HKH) on Greenland and Ny Ålesund (NyÅ) on Svalbard. The comparison is made using, to the author's knowledge, a new method; by taking the pressure difference between the two locations it is possible to get an approximation on the direction of the wind in the strait, and thereby on the dominating force of direction of the ice. A positive pressure difference and thereby a south going wind, will indicate a transport out of the Arctic Sea and more ice present along the east coast of Greenland [13]. The sea ice extent depends on the ice drift controlled by the wind forcing and due to pressure differences. Thus the ice extent is expected to be correlated with the pressure difference.

By studying a specific time of the year it is possible to get a better perspective of the year-to-year variability. This study therefore focuses a lot on the extremes; the annual ice extent minimum around 1st of September and the annual maximum around the 1st of March. The ice extent on those days are compared with the mean pressure difference for various time intervals, i.e. during the previous month, three-months and six-months period. This is done to try and find a perfect fit relative the expected displacement between the ice extent and the pressure difference.

The east coast is again divided into three parts to study variations in the correlation strength as well as the possibility of a time delay between the different regions and the effect of the pressure difference across the strait. There is expected to be various degree of correlation between the mean pressure difference calculated for the three time intervals and the sea ice extent of the different regions along the east coast. The region to the north should better coincide with the shorter time intervals of mean pressure difference and the region to the south with the longer intervals, i.e. the six-month period, due to the time it takes for the ice to get transported all the way down along the east coast of Greenland. It is expected that there is a difference between the rate of the fit for the annual minimum and maximum periods relative the mean pressure difference. During the summer there is practically no new ice formation and the ice extent is more controlled by the ice drift, thus the correlation with the mean pressure difference is expected to be better for the minimum than for the maximum.

1.3. Outline

To be able to interpret the results of this study it is important to have some background knowledge about sea ice and satellite remote sensing, both of which are very complex and vast areas of knowledge. This bachelor thesis provides a cursory overview of both areas with focus on what is considered the key parameters for this particularly study. First of all the areas of interest are presented and their main oceanographic and meteorological features are discussed, such as the three-layer structure, the ocean currents, dominating pressure systems and the impact of the sun. Some basics on sea ice are presented, i.e. formation/deformation, growth/melt, thickness, drift, distribution, heat budget, classification and snow cover. In terms of satellite remote sensing the different sensor types are discussed, with emphasis on the sensors in the microwave bands and specifically on the active synthetic aperture radar. This is followed by an overview on microwave properties of sea ice, which is of great importance for this study since they determine the outcome of the sensor signals and the received data.

2. The Greenland and Arctic Oceans

2.1. Oceanography

The Arctic Ocean is divided into the Canadian and the Eurasia Basin, which have a depth of about 4000 m and are separated by the Lomonosov Ridge. The Arctic Ocean is like the Mediterranean an almost closed off basin, surrounded on all sides by land and shallow continental shelves, which cover a vast area of the Arctic Ocean. The shelves reache out 600 km from the shore and the shallow seas, such as Barents, Kara, Laptev, East Siberian and Chukchi (see figure 2.1a), have depths of <100 m. These shallow seas limit the exchange between the Arctic Ocean and the oceans around. The only deep passage present is to the Atlantic Ocean between Greenland and Svalbard, the Fram Strait. The Strait is about 600 km wide and has a depth of 2600 m and accounts for almost all the water and heat exchange with the Arctic Ocean. There are a few shallow straits as well such as the Bering Strait towards the Pacific Ocean and the narrow Nares Strait to Baffin Bay as well as many links through the Canadian Archipelago and Barents Sea [7].

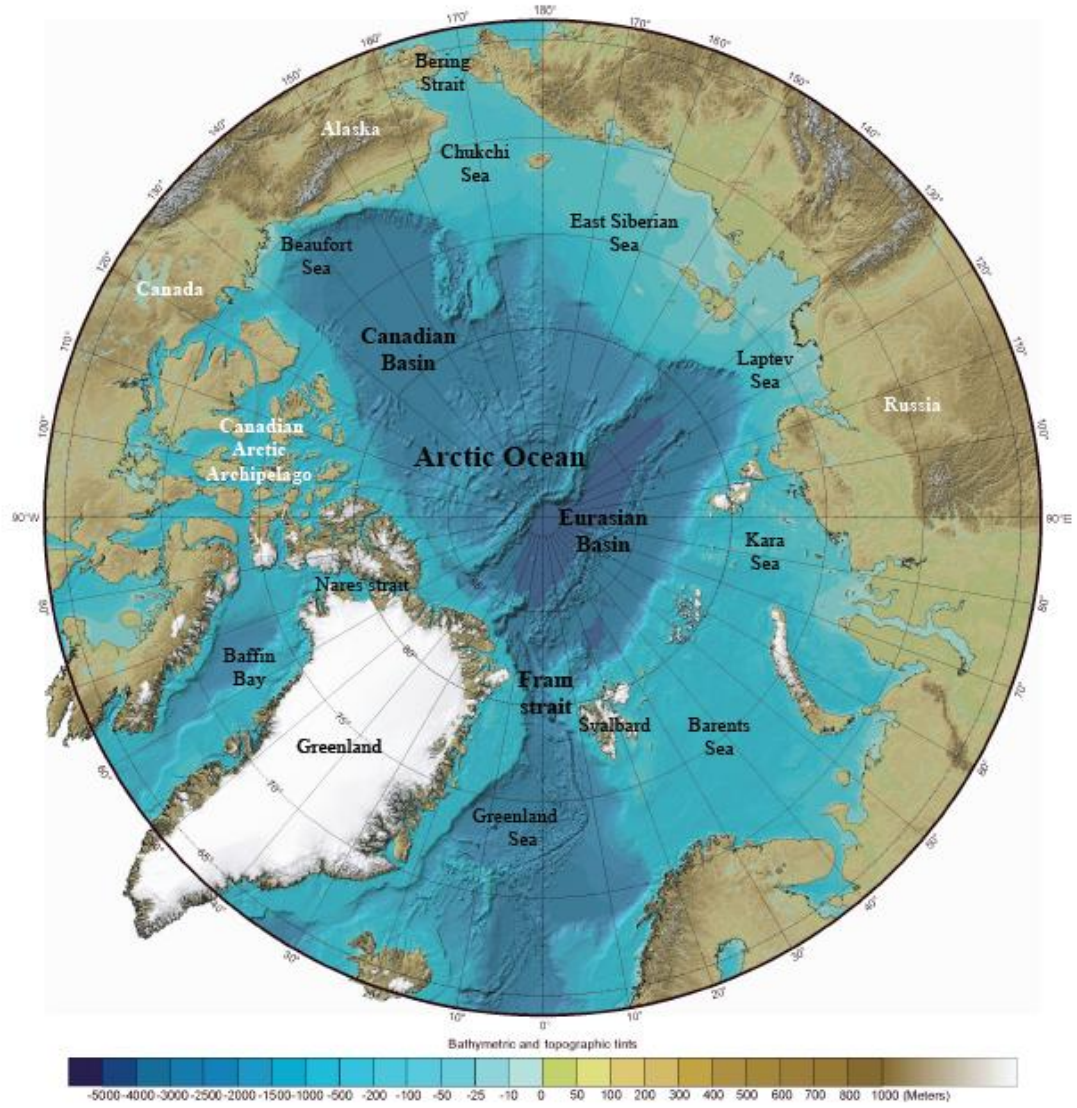

Figure 2.1a. The international bathymetric chart of the Arctic Ocean, modified by M.Brandt Jensen originated from IBCAO [5, 14]

The water column of the Arctic seas can approximately be divided into three different types: the *polar surface water*, the mid-layer *Atlantic water* and the *Arctic Ocean deep water* (see figure 2.1b). The polar surface water is very cold, near the freezing point of -1,86ºC, and has a low salinity of 30-32 psu. The low salinity is due to the massive influx of freshwater to the Arctic Ocean through large river systems on the North American and Asian continents [7]. Below the polar surface water, at mid depths of 200-900 m, is the Atlantic water which has a higher temperature of 3ºC and a higher salinity of 35 psu. This layer of water originates in the Atlantic and is transported into the Arctic through Fram Strait and Barents Sea at mid depth due to its higher density. At the bottom of the water column is the Arctic deep water which has about the same salinity as the Atlantic water but a lower temperature of -1-0ºC. The deep water originates from sinking water in the central Greenland Sea which is then transported into the Arctic basins [7, 15].

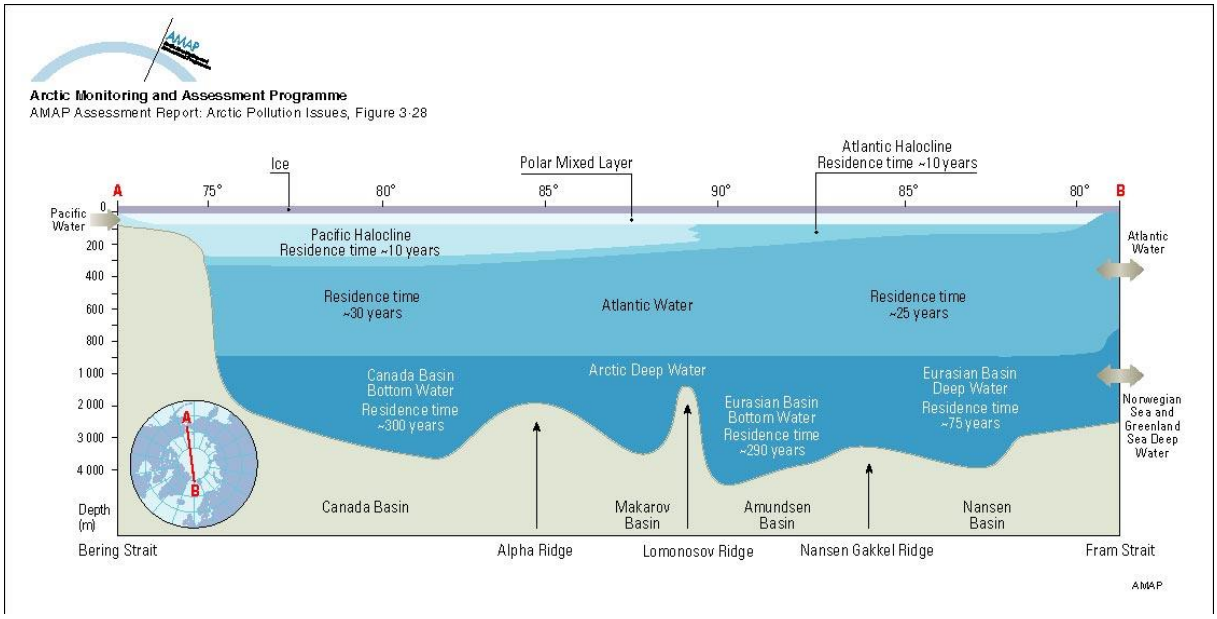

Figure 2.1b. A schematic representation of the three-layer structure of the Arctic Ocean, with the polar surface water above the Atlantic water and Arctic deep water. The residence time for the different water masses are also shown [16].

The three layer structure gives rise to a very stable water column which makes the chance of mixing small, thus the formation of new deep water very slow. However, during the winter the density differences between the layers are relative small in the Greenland Sea, due to atmospheric cooling of the surface water along with the formation of new ice. The cooling makes the surface water colder than the layer below and the ice formation increases the salinity, resulting in a very dense surface layer and a possible mixing situation. The input of fresh water, i.e. the amount of ice transported by the East Greenland Current determines the rate of the convection (see figure 2.1c) [15].

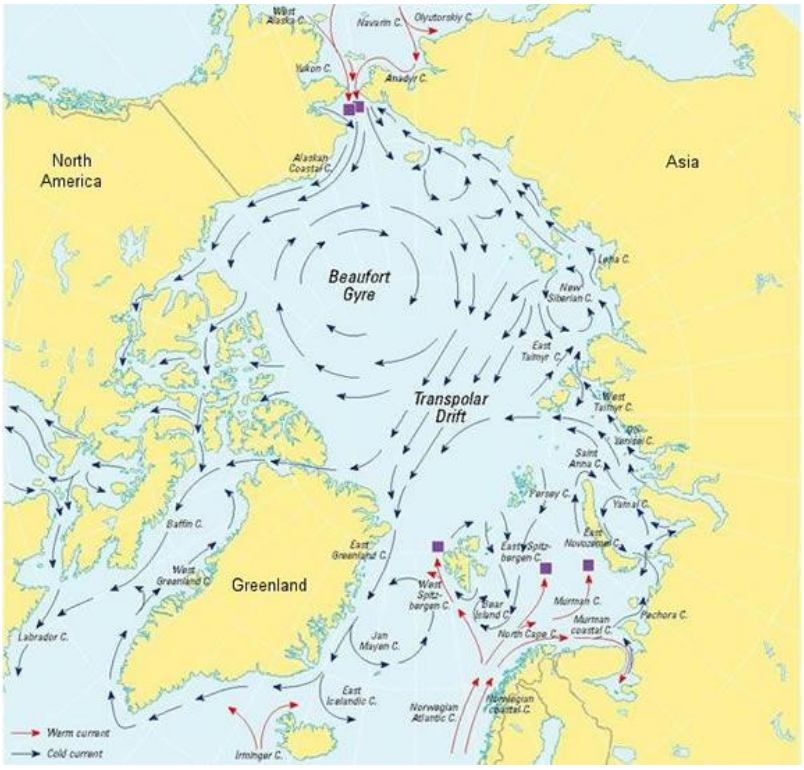

Figure 2.1c. Arctic Ocean surface circulation, where blue arrows indicate cold polar surface water and red warmer Atlantic water. The square boxes show where the Atlantic water sinks and flows under the colder polar water. [16].

In an ice covered ocean, like the Arctic Ocean, the long-term motion is the same for surface water and ice, meaning the mostly wind driven surface currents of the Arctic control the direction of both the surface water and the ice drift. The surface current system of the Arctic Ocean is dominated by the anticyclonic circulation in the Canadian Basin, the Beaufort Gyre and the Transpolar Drift Stream in the Eurasia Basin (see figure 2.1c) [7]. Within the Arctic the ice drift is relatively slow and the anticyclonic Beaufort Gyre, centred in the Beaufort Sea, may circulate ice floes for several years before they melt or get caught up in the Transpolar Drift Stream. The Drift Stream transports water and ice from the shallow continental shelves of Asia, across the ocean towards Greenland, within about three years. As the current enters through Fram Strait the drift speed generally increases and is renamed the East Greenland Current [17].

The very cold East Greenland Current which is the major transporter of sea ice out of the Arctic Ocean, continues down the coast of Greenland. It is more or less sharply delimited on the outside by branches of the North Atlantic Current, which has moved up along the coast of Norway. The East Greenland Current continues as a mixed flow as the two water masses are gradually combined and rounds Cape Farewell. The Atlantic water sinks and enters the Arctic predominantly as the West Spitzbergen Current at mid-depth, as illustrated in figure 2.1c and 2.1d [15, 18].

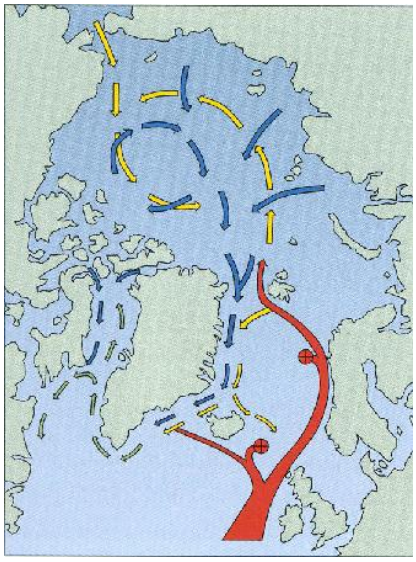

When passing through the Greenland Sea the East Greenland Current recirculates as the East Island and Jan Mayen Currents. Especially the latter may generate additional new ice formation and give rise to an ice peninsula stretching out like a tongue; the phenomenon is known as Odden (note that the Odden has not been observed in the past few years) [4].

Figure 2.1d. Sea currents in the Arctic Ocean and the North Atlantic Ocean. The polar water flows like a cold, icy current southward along the east coast of Greenland. The warm North Atlantic Current flows north and sends out branches in the direction of Greenland, and parts of it sink to mid-depth (marked with an ⊕) [18]

2.2. Meteorology

The atmospheric conditions of the Arctic region are controlled by large-scale pressure systems which are more prominent during the winter months, see figure 2.2a. In the winter the surface pressure situation is dominated by the semi-permanent Islandic low, between Island and Greenland, stretching out into the Barents Sea as well as the Arctic high. The Arctic high refers to a quasi-permanent high in the Beaufort Sea connected to both the strong continental Siberian high and the Greenland high. Together these pressure systems create strong surface pressure gradients during the winter, resulting in strong winds. The winds, which move along the isobars, generate an anticyclonic circulation around the Beaufort high, the Beufort Gyre, and a motion across the Arctic seas, the Transpolar Drift Stream. The strong quasi-permanent pressure systems weaken during the spring and in the summer the pressure is lowest in the central Arctic Ocean. The pressure situation may even generate cyclonic winds in the Beaufort Sea and the Arctic Ocean, however the average motion of the ocean is anticyclonic [17].

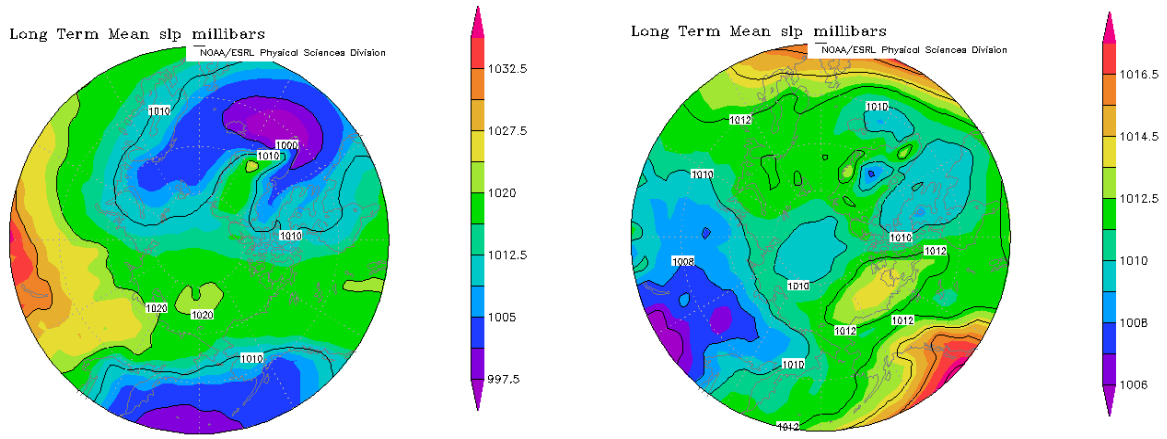

Figure 2.2a. Mean sea level pressure in the Arctic 1981-2010, monthly mean dec-feb and june-aug [19].

The pressure patterns in the Arctic use to vary opposite that of 45ºN, close to the Azores, i.e. high pressure in the Arctic region generally coincides with low pressure at mid-latitudes and vice versa. This oscillation is called the *North Atlantic Oscillation* or the *Arctic Oscillation*, which are just two slightly different ways of describing the same phenomenon. The North Atlantic Oscillation is a comparison between the Icelandic low and the Azores high while the Arctic Oscillation compares the Arctic high with the pressure at mid-latitudes. The oscillation ranges on a time scale from weeks to decades and it extends through the depth of the troposphere, strongest during the winter. The Oscillations control the strength and direction of westerly winds and the route of cyclones travelling across the Atlantic Ocean [20].

When the Arctic Oscillation is in a positive phase, i.e. low pressure in the Arctic and high pressure in the mid-latitudes, the Beaufort high as well as the Beaufort Gyre is weakened. This results in strong and consistent westerly winds, thus the cold polar air gets trapped in the Arctic region providing cold and dry weather. When the Arctic Oscillation is in a negative phase (see figure 2.2b), i.e. high pressure situated in the Arctic and low in the mid-latitudes, the zonal winds are weak and exchange of air between the North and South is possible. The cyclones travel further north, advecting cold polar air down south and hot and moist air up north, resulting in relative warm and stormy weather in the Arctic region [20].

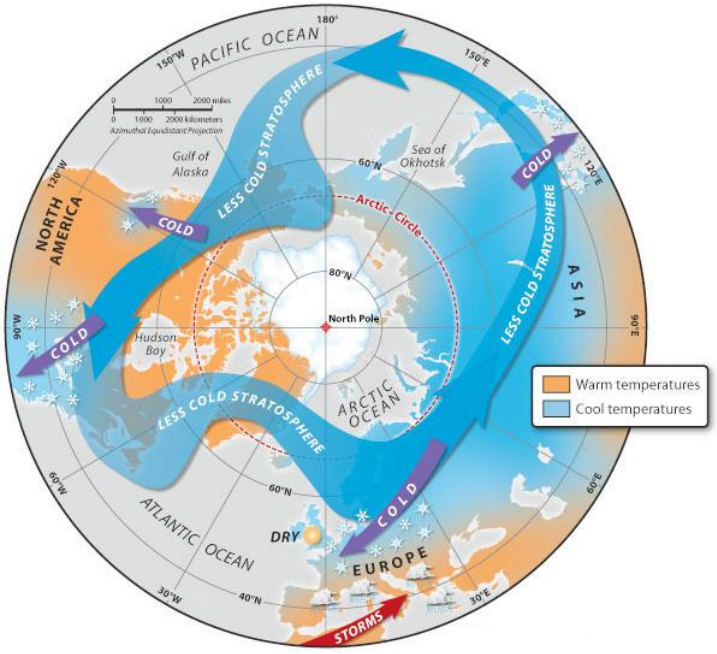

Figure 2.2b. The Arctic Oscillation in negative phase creates weak winds, colder weather outside the Arctic and more heat and moisture in the Arctic region. Image created for the Smithsonian's National Museum of Natural History [21].

Oscillations such as the North Atlantic Oscillation and the Arctic Oscillation control the weather situation in the Arctic over longer time scales while cyclones and short lived polar lows, frequent in the Greenland sea, dominate on a shorter time scale as they transport heat, moisture and momentum into the region. The Greenland landmass reaches about 3000 m up into the sky, resulting in an atmospheric blockage and a high impact on the air exchange between the North and South as well as on movement of the pressure systems. The low tracks are forced around the big island and as they pass along the coast they may give rise to local

weather phenomenon such as the katabatic wind. The katabatic wind may blow with unaltered speed almost 200 km off the coast of East Greenland [15].

In the polar regions the surface temperature is highly affected by the latitude and the insolation. Due to the tilt of the Earth there is a time when the sun does not set in the region north of the Arctic Circle, called the *polar day*. This period of time increases from the Arctic Circle, where it is just one day, towards the North Pole where the sun rises in the spring and does not set until autumn. When the sun sets on the North Pole it is covered in complete darkness for six months until the sun rises around the spring equinox. This results in significant seasonal variations in solar fluctuation and thereby temperature [20].

The central Arctic is very dry and precipitation is sparse, especially in winter when the ice cover is thickest. In some places the air is as dry as in the Sahara desert and the inner Arctic is often referred to as a *polar desert*. There is little evaporation from the ocean except in openings in the ice and along the sea ice edge [20]. Over the ocean and along the ice edge heat and steam are released from the ocean and fog and clouds form, they are said to cover the sea ice edge of the Arctic up to 70% of the time [23].

3. Sea Ice

Sea ice (figure 3a) forms in the cold polar regions and covers an average of 7% of the entire world ocean surface in the annual mean; this study focuses exclusively on the North Pole and the surrounding seas. At the sea ice annual maximum extent in March the sea ice covers about 5% of the Northern Hemisphere [1, 22, 23].

Figure 3a. Sea ice forms in the cold polar regions, such as the North Pole [24].

Sea ice is an important and sensitive indicator as well as modulator for the global climate system [23]. The sea ice works as an effective insulator for heat, gases and momentum exchange between the ocean and the atmosphere. The heat flux through open water is twice that through thick ice [25]. The sea ice also has a significant impact on the global climate system through the ice albedo feedback mechanism, see figure 3b [1]. Sea ice and snow has a higher reflectivity than open water, with an albedo of about 80% in contrast to the waters 10-20% [22]. This effect is especially apparent in the summer, when the insolation is high [25]. The sea ice also plays a major role in the global sea circulation. Via rejection of salt during growth and the transport and input of freshwater during melting the sea ice creates convection in the oceans [25].

Figure 3b. The ice albedo feedback mechanism, the incoming sunlight reflects on the ice but is absorbed by the ocean which has a lower albedo [26].

3.1. Formation and snow cover

During the winter the ocean looses a lot of heat to the atmosphere through areas of open water. When the ocean reaches a temperature of -1,86ºC, at a salinity of 34 psu, the top layer of the ocean start to freeze [17]. The ocean forms small needle-shaped ice crystals called *frazil ice*; these ice crystals accumulate at the ocean surface and binds together to form ice sheets [27].

When the frazil ice crystals form, salt accumulates into droplets called *brine*. The saturated salt droplets are mostly rejected back to the ocean but some are trapped between the freezing ice crystals. With time the brine drains out, leaving air pockets, either with the help of gravity or melt water flushing through cracks in the ice [27]. Brine has a lower thermal conductivity than pure ice, by a factor of four, thus the thermal conductivity of the ice sheet is mainly determined by the amount of brine [17].

In calm seas the frazil ice forms thin and smooth ice sheets which, after covering the surface and blocking the heat flux to the atmosphere, grows by ice crystals forming underneath. The crystals forming below the ice sheet are called *congelation ice*, and they are much longer and smoother than the frazil ice crystals [23, 27]. Frazil ice formed in rough waters on the other hand quickly freeze together to form near-circular ice, called *pancake ice*. The ice discs will eventually attach themselves to each other, damping the wave motion and finally freeze together to a somewhat thick and rough ice sheet [23, 27]. These different stages in the development and formation of sea ice are showed in figure 3.1, for a more detailed description see Eicken (2003) and Wadhams (2000).

With time the ice cover may accumulate a snow cover, though it is only in the pack ice margin that the precipitation is significant. The interior of the Arctic is much like a frozen desert, making the snow cover of the inner pack ice only a few centimetres thick. Snow is a much stronger insulator than ice, as discussed in section 3.3; though the snow cover only accounts for about 10% of the total mass of ice in the polar region, it still has a major impact on the heat budget [17]. Snow albedos are much higher than those of bare ice, which makes the snow cover control the shortwave energy exchange (i.e. the range in the visible spectra where the sun has its maximum) and the ice albedo feedback mechanism [23]. The feedback mechanism means that a warmer climate results in less ice and thereby more heating by incoming shortwave radiation, due to lower albedo of the open waters.

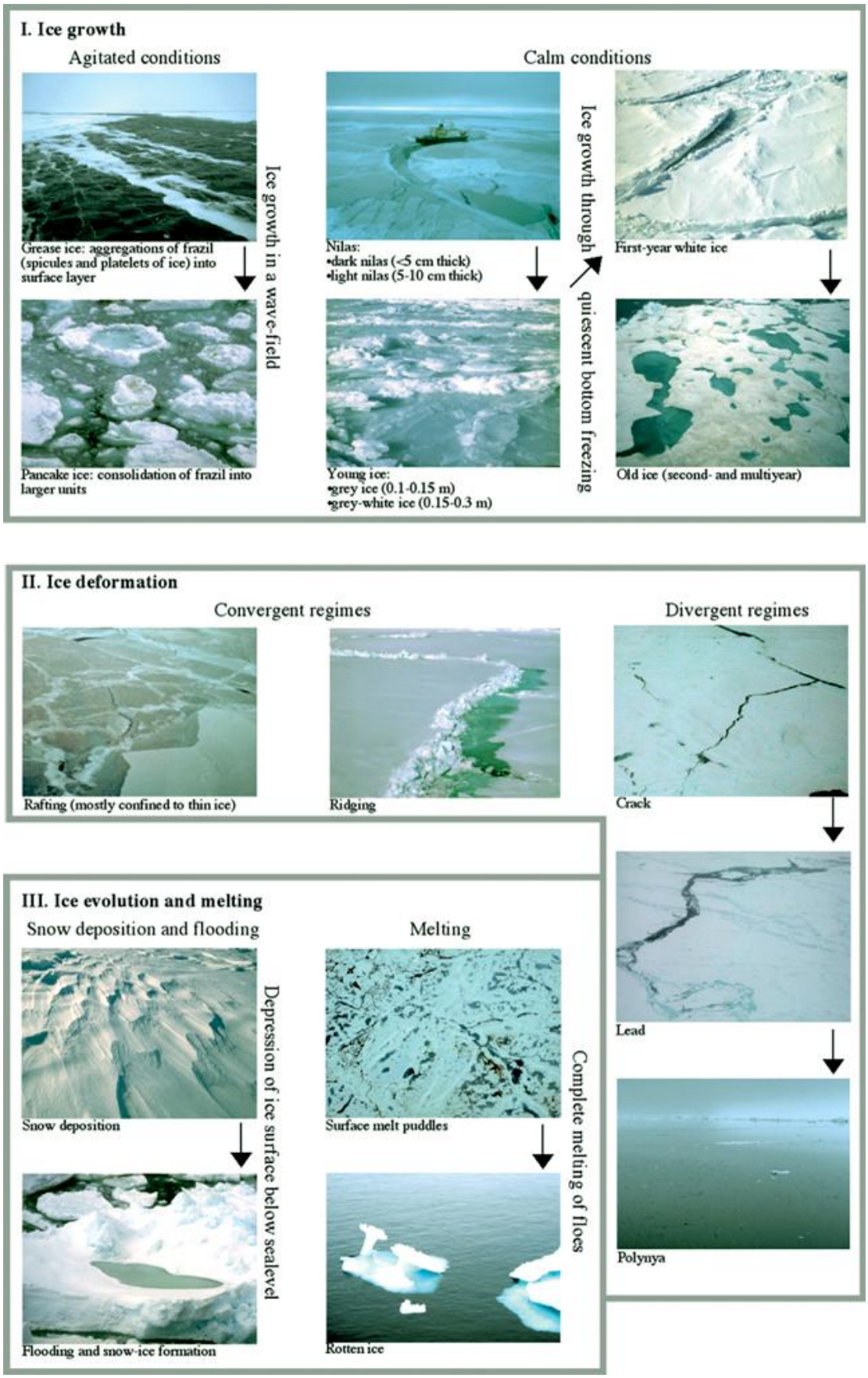

Figure 3.1. Sea ice types, pack ice features and growth, melt and deformation processes [17].

3.2. Deformation, thickness and drift

Sea ice is highly mobile, it drifts and deforms in response to synoptic-scale changes in wind, tidal forcing, altered ocean currents, internal ice stress and sea surface tilt [27]. The forces acting on the ice might be either divergent or convergent, see figure 3.1. Divergence gives rise to open-water areas within the pack ice where new ice can form. The open areas are called *leads* if they are linear and short-lived and *polynyas* if they are long-lived due to turbulence in either the ocean or the atmosphere [23]. Convergent forcing gives rise to deformation and thickening of the ice sheet. The ice sheet might break up in smaller ice *floes* which can *raft*, i.e. glide on top of each other, and *ridge*. Ridging means that the ice floes, after given way to the pressure, get piled on top of each other (see figure 3.2a). The ridging will create a much thicker ice sheet than the rafting, up to tens of meters of which most of the ice is under the surface like a keel [23]. The thicker the initial ice sheet the bigger the chance of ridging instead of rafting [17].

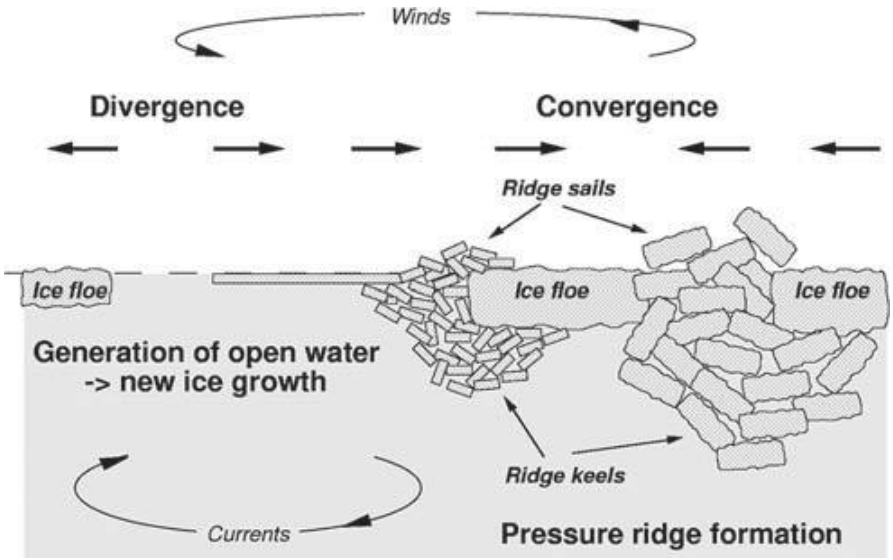

Figure 3.2a. Illustration of the processes that dynamically, i.e. by divergent or convergent ice motion and deformation, modify the ice thickness distribution [28].

The deformation process depends on the thickness of the ice, thin ice is more compressible than thick ice, making it easier to deform by convergent motion. Thus thin ice can increase the thickness and rapidly decrease the sea ice extent in an area experiencing external forces, such as strong winds [29]. The amount of energy transported from the atmosphere to the sea ice depends on the stability of the atmosphere, the surface wind velocity and the surface roughness (thick and old ice often have a rougher surface than young and thin ice) [23].

On a short-term timescale the free drift of the sea ice, i.e. away from coastlines and other anchor points, is highly correlated with the geostrophic wind. In the Arctic, the sea ice drifts at ~1% of the mean geostrophic wind speed and at an ~18º angle to the right [23]. Over longer timescales such as several months and years the sea ice moves mainly in responds to the atmospheric circulation and the ocean currents. In the Arctic, the sea ice drift is dominated by the anticyclonic Beaufort Gyre and the Transpolar Drift Stream, which transports the ice across the Arctic basin towards Greenland and the Canadian archipelago (see figure 2.1c). When the sea ice is pushed towards the coastlines it creates a high internal stress, which makes the ice deform and create massive ridges which accounts for the thickest ice in the polar oceans (see figure 3.2b)[28].

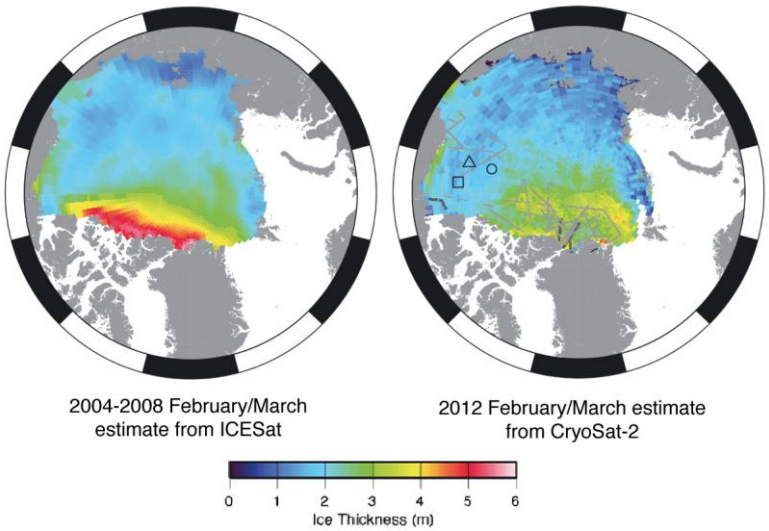

Figure 3.2b. Images of estimated sea ice thickness from satellites during February-March, 2004-2008 and 2012. The figures and gray lines in the right images are data collected for validation [30].

Ridges may contain as much as 30-80% of the total ice volume in a measured area, making it hard to estimate the thickness. An alternative method is to calculate and compare the amount of first-year and perennial sea ice, as they differ in thickness [23].

3.3. Heat budget and decay

Heat reaches the ice through shortwave radiation during the summer and through heat conductivity from the deep ocean, accumulated predominantly during the summer through radiation absorbed by the ocean [7]. Ice growth and melt are controlled by heat fluxes in and out of the upper and lower sea ice interface, which in turn are controlled by the thermodynamic properties of the snow and ice cover [23].

Snow has a lower thermal conductivity and diffusivity than sea ice, making it a stronger insulator. The snow has a conductivity of about 0,2 $Wm^{-1}K^{-1}$, compared to the conductivity of sea ice which is about 2 $Wm^{-1}K^{-1}$, and can reduce the conductive heat flux through the ice by up to 50% [17]. During freezing conditions heat is extracted both by cooling the interior of the ice and by the formation of new ice below the existing ice sheet. The heat is transported upwards through the ice at a rate dependent on the conductivity of the ice and snow cover as well as the heat balance at the lower and upper ice surface [23].

The thickness of the snow and ice cover determines the conductive heat flux through the ice cover and thereby the ocean-atmosphere heat exchange, which effects the thermodynamic growth and melt rate. Thus the thicker the ice, the lower the rate of the thermodynamic ice growth. During winter massive amount of heat are lost from the ocean to the atmosphere through thin ice, cracks and openings in the sea ice, resulting in a substantial ice growth [23]. The ice can only grow to a certain thickness, called *thermodynamic equilibrium thickness* (about 3 m in the Arctic), before it gets too thick and the conductivity too low for the heat to transfer through it [27]. The heat will get trapped under the ice, preventing it from growing and eventually melting it from below; note however that the ice can still get thicker due to external forcing and deformation [17].

A snow cover delays the melting of an ice sheet due to its high albedo and low thermal diffusivity [23]. The melting of the snow begins in June and the melting of the ice at the end of the month, thus the snow cover gives the ice an extra month [7]. The insolation, in the spring and summer, increases the temperature at the top of the ice interface and makes the upper layer of snow and ice melt. The melting water accumulates in *melt ponds* which has a much higher albedo than the ice and snow, thus it creates a positive feedback process by increasing the heating of the surface. Insolation has an immense effect on the Arctic sea ice and melt ponds may cover as much as 60% of the Arctic sea ice area in the summer [23].

3.4. Classification and distribution

The sea ice is divided into different categories depending on the properties and different steps in the aging process. First of all the ice cover is divided into *fast ice* and *pack ice*, the first being ice attached or frozen to the coastline and the latter being mobile floating sea ice entirely free from the shore [31]. Ice cover less than one year old is called *first year ice* and it is 0,3-2 m thick. An ice cover that has survived more than two annual summer melt are called *multiyear* or *perennial sea ice*, and is characterised by a thickness of more than 2 m and a much lower salinity than the first-year ice. This thick ice cover has an efficient drainage system for melting water and contains a lot more air bubbles than the younger ice, due to brine drainage. The interior of the Arctic pack ice consist of mostly first year sea ice, which in general has a smoother surface than the multiyear ice. However, the thin first year ice has many sharp ridges due to deformation processes, while the multiyear ice is more like a moonscape due to several years of external forcing by the elements [17].

The *sea ice edge* is where the ice meets the open water and its location is determined by the air temperature, wind speed and direction and ocean heat flux as they influence the ice drift and growth rate [17]. Within the margin of the ice edge the sea ice concentration are measured in tens, according to the WMO Sea Ice Nomenclature, and divided into different area elements, where 0/10 are open water and 10/10 are compact pack ice. The ice edge may therefore be compact or diffuse, going from solid ice to open water or stretching several kilometres with a few ice floes. The ice *extent* is the sum of all the area elements where the concentration is above 1-2/10, i.e. more than 15%, and the sea ice *area* is the "actual" ice covered area. The sea ice area is calculated by multiplying each area element with its concentration and add them together [31].

At the sea ice annual maximum extent in March all of the Arctic Ocean is covered by ice as well as most of the adjacent seas; Barents, Kara, Beaufort, the Canadian Archipelago and Baffin Bay. The ice also extends through the Bering Strait, down the coast of Russia and through Fram Strait down the east coast of Greenland. During the annual minimum ice extent in September the ice covers the inner of the Arctic Ocean, the Canadian Archipelago and the northeast coast of Greenland [DMI, 27].

4. Satellite Remote Sensing

Unless otherwise stated, the information and the figures in this chapter come from Lubin and Massom (2006) [23].

By the use of satellite remote sensing it is possible to measure the variability of the inaccessible sea ice and its extent in the Northern Hemisphere. Remote sensing of sea ice, from polar orbiting satellites, is based on the interaction between electromagnetic radiation, the ocean surface and the snow and ice layers. The interpretation of the physical sea ice properties received from the emitted, reflected or backscattered radiation depends on the surface and instrument characteristics, i.e. surface topography and roughness, wavelength, polarization and incident angle. There are two types of sensors, passive and active; the first receives emitted thermal radiation (middle infrared and microwave) or reflected solar radiation (shortwave radiation) and the latter emits its own radiation and receives the reflected energy. The first polar orbiting satellites with this type of equipment were launched in the late 1970s and have since then provided an unbroken record of sea ice data. In the present study data from active sensors are used to study the sea ice extent along the east coast of Greenland while data from passive sensors are used for the extent in the entire Northern Hemisphere.

4.1. Basics

The imaging instruments onboard the polar orbiting satellites are sensitive to *electromagnetic radiation* and gives information about surface properties, i.e. roughness, emissivity and thereby type of ice and approximate thickness. The sensors only use fractions of the electromagnetic spectrum, a few specific wavelengths, called bands (see figure 4.1a). These bands have a high atmospheric transmission, i.e. the radiation can pass through the atmosphere without being absorbed by gases such as water vapour, carbon dioxide and ozone. The high transmission bands are referred to as *atmospheric windows* and the low transmission bands as *atmospheric absorption bands*. As can be observed in figure 4.1a the microwave bands are within the region of the biggest atmospheric window and are therefore a beneficial sensor type.

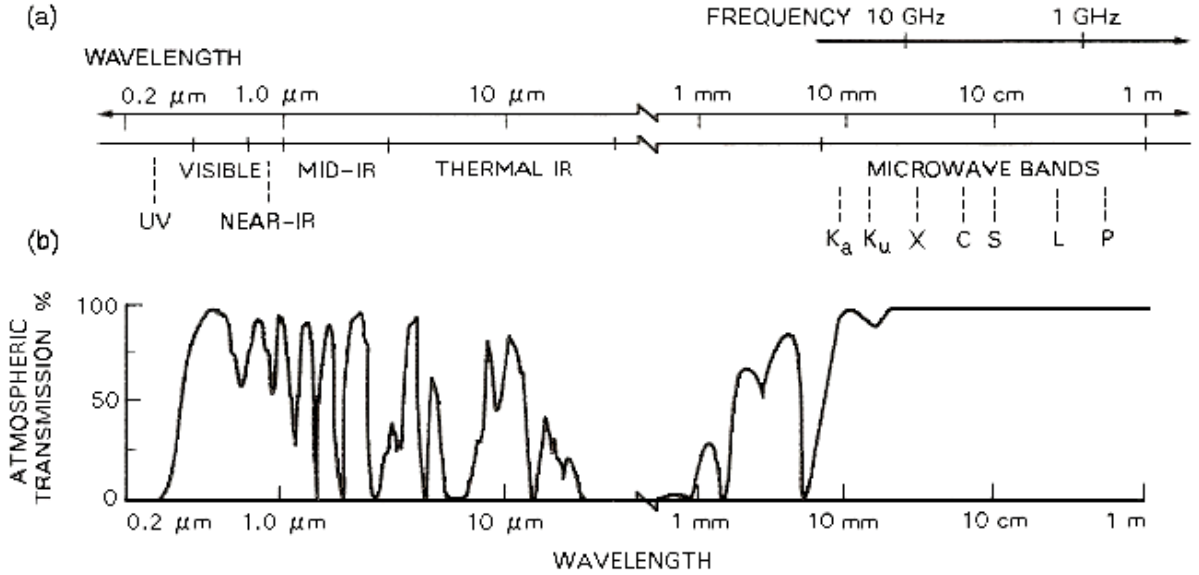

Figure 4.1a. (a) The electromagnetic spectrum with the major sensor classes marked. (b) A plot of atmospheric transmission as a function of wavelength.

The sensors receive the electromagnetic radiation within their specific band of wavelength that has been emitted, reflected or backscattered by the surface and has interacted with the atmosphere, see figure 4.1b. The measured energy gives an average intensity which in turn is converted to a *brightness temperature* or radiant temperature, i.e. the actual temperature emitted by the surface times the surface emissivity. The resulting measurements are recorded by the sensor and the data are displayed digitally for further visual and numerical interpretation [32].

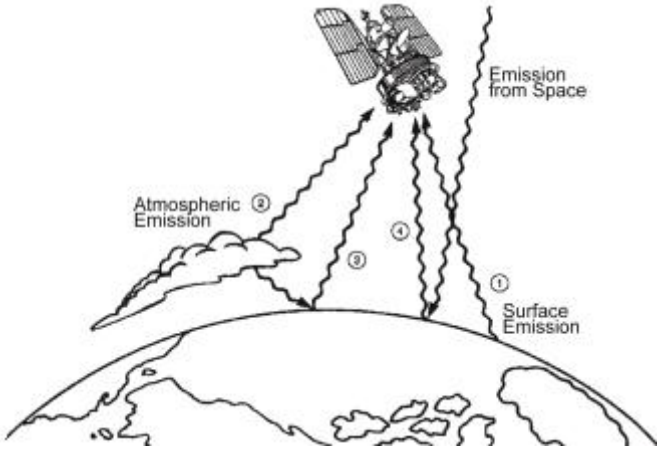

Figure 4.1b. The satellite carried sensors receive emitted, reflected and backscattered radiation from the earth and the atmosphere which together form the brightness temperatures [4].

The two most important properties of the sensors and what mainly determines their efficiency and accuracy is the *swath width*, and thereby the *footprint* (i.e. the geographical area affected by the radiation), as well as the sensor *resolution*. The sensors are very limited, all of them have their strength and weaknesses and at the moment there is no ideal, all-purpose sensor. A good resolution leads to a smaller swath with, due to several technical difficulties, i.e. a sensor with medium resolution of >250 m can have a swath width of >1 500 km while a sensor with really high resolution <5 m can have a swath width as low as 10-20 km. At the high altitudes of the Arctic the interval of passing is also determined by the swath width, the wider the swath the shorter the revisit interval. To get images of a specific desired spatial and temporal resolution there is a range of datasets that may be put together (see figure 4.1c).

Spectral range	*Wavelenght*	*Quantity measured*
Visible		
Blue, green, red	0.4-0.73 μm	Reflectance
Infrared		
Near-IR	0.7-1.3 μm	Reflectance
Mid-IR	1.3-3.0 μm	Reflectance + Thermal emmision
Thermal IR	3.0-5.0 μm, 8.0-14.0 μm	Thermal emmision
Microwave	1 mm – 1 m	
Passive		Thermal emmision
Active		Reflectance

Figure 4.1c. The spectral range of divisions of the electromagnetic spectrum exploited by satellite remote sensing.

4.2. Passive sensors

As mentioned before there are several different types of sensors, most of them are passive as can be seen in figure 4.1c. The *passive sensors* cover almost all the electromagnetic spectrum; there are optical imagers, operating in the visible spectrum and depending on reflected sunlight and clear skies, such as MODIS. There are sensors in the near-infrared and infrared (IR) part of the spectrum that only can operate during clear sky conditions, like the AVHRR. The IR sensors measure emitted thermal radiation which makes them unaffected by the absence of sunlight and able to operate during the night. There are several different types of passive microwave sensors; they are unique among the passive sensors in the way that they can penetrate clouds and operate in any weather conditions. Clouds roughly absorbs most of the radiation with wavelengths <0,9 cm, which makes the microwave bands the only ones able to penetrate them. Like the IR sensors the microwave sensors measure thermal radiation and are thereby capable of providing data all day, all year round. Two such passive microwave sensors are the SSMR and the following improved SSM/I, of which the latter will be further discussed in the following chapters as it is of importance for this study. The two passive microwave sensors provide the most consistent and complete sea ice data available, since the launch of the carrying satellite of SSMR in 1978.

4.3. Active sensors

Active sensors, so called *radars*, are an important resource due to their capability of penetrating clouds; they can operate as usual regardless of weather conditions. They emit their own electromagnetic radiation and measure the intensity and characteristics of the reflected or backscattered radiation. The emitted radiation is able to penetrate the ice surface to provide information on internal properties and thereby making it possible to determine the type of ice as well as its stage of development. The strength of the backscattered radiation depends on both surface and internal properties as well as radiation frequency, angle of incidence and polarization. There are three types of active microwave sensors, the *synthetic aperture radar* (SAR) which is illustrated in figure 4.3, the radar *scatterometer* and the radar *altimeter*. Since SAR is the only one used in this study it is also the only one who will be further discussed.

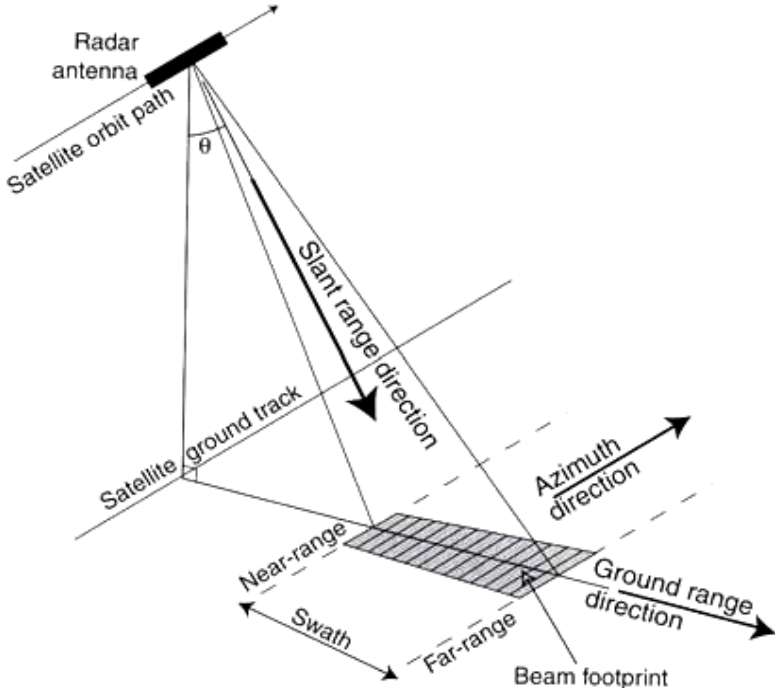

Figure 4.3. Illustration and main terms of satellite SAR geometry [33].

4.3.1. Synthetic aperture radar (SAR)

SARs have a very high resolution (tens of metres) due to their use of relative motion between the sensor and the observed object, making it possible to map specific small scale ice formations such as leads, polynyas and pressure ridges. They have however a very small footprint which gives a limited temporal coverage. The sensors are also sensitive towards contamination from atmospheric water vapour effects, particularly in summer and at shorter wavelengths.

4.4. Microwave properties of sea ice

The intensity of the received microwave radiation is determined by the scattering (*geometrical*) and material (*dielectrical*) properties of the sea ice in interaction with the wavelength, polarization and incident angle of the sensor. It is essential to have knowledge about basic sea ice microwave properties to be able to understand and interpret sea ice data from satellite remote sensors.

The backscattering properties of the sea ice highly depend on the dielectrical characteristics, i.e. the amount of brine and air bubbles within the ice. The sea ice *dielectrical constant* depends on the varying composition of the three elements: pure ice, brine and air. A high dielectric constant is equivalent with high concentrations of brine and a low penetration depth, resulting in mostly surface scattering.

Depending on the geometrical characteristics of the surface, i.e. the roughness, the surface tends to reflect the radiation differently. In general, a rough surface acts like a *diffuse reflector* and reflects the radiation in all possible angels while a smooth surface acts like a *specular reflector*, that is the outgoing radiation has the same angle as the incoming, see figure 4.4. The rough surfaces therefore have a higher amount of backscatter and appear to be brighter, such as multiyear ice which has deformed over time. The multiyear ice also has lower bulk salinity

than first-year ice which makes it more like pure ice, i.e. giving it a low dielectric constant and a high penetration depth. This results in a predominant *volume scattering*, meaning multiple scattering within the ice as illustrated in figure 4.4. First-year ice on the other hand has high bulk salinity, thereby a low dielectric constant and the scattering mechanism is predominantly surface scattering. All these effects make multiyear ice look bright and first-year ice slightly darker.

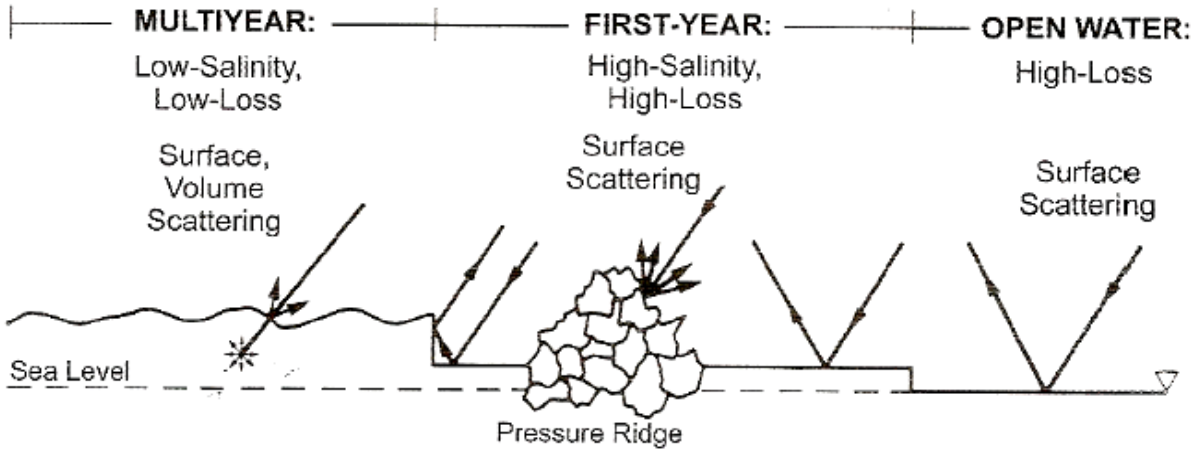

Figure 4.4. A schematic of idealized radar backscatter interactions with smooth open water, smooth first-year ice, pressure ridges, floe edges and Arctic multiyear ice.

The microwave radiation is sensitive towards water; the higher water content on the ice surface (or in the atmosphere) the higher the dielectric constant which changes both the albedo and the rate of absorption. With more water the microwave penetration depth will decrease, making surface scattering the dominant reflection mechanism. The annual variations in melting and freezing, i.e. variations in the water content, may significantly change the brightness of the surface and make the analyse difficult. That is why the absence or presence of a snow cover may be the determining factor of the microwave signal. The density of the snow cover may vary rapidly on a very short vertical scale on the sea ice and the amount of liquid in the layer may alter the radiation. The surface albedo is also highly controlled by the snow cover; multiyear ice with a snow cover has the highest albedo while bare first year ice has the lowest, i.e. except for the melt ponds and the open ocean.

5. Data

In this study the variability of the sea ice extent is analysed during the period 2000-2012. Manually produced ice charts of the ice extent, from the Danish Meteorology Institute (DMI), over the east coast of Greenland are compared to the ice extent data from passive microwave data over the entire Northern Hemisphere. The variability of the ice extent is also compared to the pressure difference between two weather stations located on either side of the Fram Strait.

5.1. Ice charts - Greenland

The ice charts are mainly produced to support navigation of ships in the supervised region [34]. They are manually produced by interpretations of a combination of different data sets, with active SAR and optical MODIS images as the primary data source. This way of connecting different forms of data creates a high resolution product (see figure 5.1a) [15].

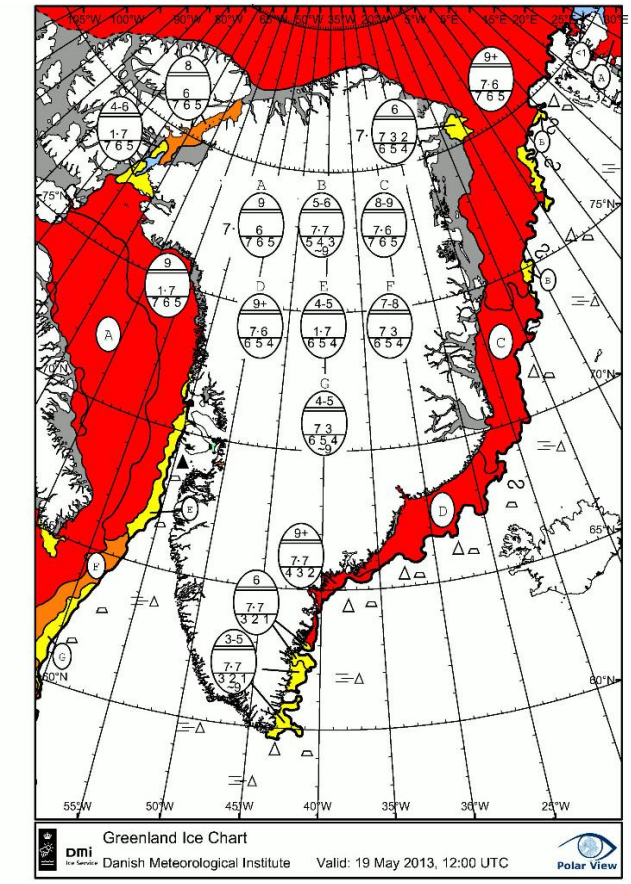

Figure 5.1a. Manually produced, Greenland overview, ice chart by the DMI showing the ice extent in the region around Greenland on the 19th of May 2013 [34].

The main data is achieved from SARs carried by different satellites; the first satellite used by the DMI was the Canadian Space Agency's (CSA) Radarsat-1 launched in 1995 and used until 2010. Radarsat-1 was able to deliver images of the earth day and night, through cloud cover, smoke and haze, and it was a real breakthrough for the monitoring of sea ice. The satellite had several different modes where the swath width ranged from 45-500 km and the resolution from 8-100 m, 25-100 commonly used for ice charting see table 5.1 [35]. Radarsat-1 was followed by the European Space Agency's (ESA) Envisat launched 2002. It was the first time

SAR data became available to a broad audience, i.e. public and for free, and Envisat became a clear favourite at DMI from which most of the data was achieved [36].

Envisat had a variable swath width of either 100 km or 400 km and an image resolution of 30 m-1 km. The contact with Envisat was lost in the beginning of 2012, after 10 years of collecting sea ice data [37]. In 2007 the Canadian Space Agency launched Radarsat-2 as a follow-up to Radarsat-1, see table 5.1. The satellite has like the others different modes and a variable swath width of 18-500 km and a resolution of 9-100 m, however the range 25-50 m in image resolution is commonly used for ice charting [35]. Radarsat-2 is still in use with some supplementary data from the Italian Cosmo Skymed which was launched in 2007 but not fully operational until 2010. In the near future ESA is planning on launching a sequel to Envisat, Sentinel-1, which will be the first in a new line of radar carrying satellites [37].

Satellite	Sensor	Swath width	Resolution	Time interval	Organization
Radarsat-1	SAR	45-500 km	25-100 m	1995-2010	CSA
Envisat	SAR	100 km and 400 km	30-1 000 m	2002-2012	ESA
Radarsat-2	SAR	18-500 km	25-50 m	2007-present	CSA
Aqua/Terra	MODIS (optical)	2 330 km	250-1 000m	1999/2002-present	EOS
NOAA	AVHRR (infrared)	3 000 km	1 100 m	1978-present	NOAA

Tabele 5.1. The main satellites and sensors used by DMI for ice charting, listed in order of appearance.

The SAR data are supplemented with optical images from MODIS, IR images from AVHRR and microwave images from SSM/I. MODIS (Moderate Resolution Imaging Spectro-radiometer) is a key instrument onboard the Earth Observing System (EOS) Terra, launched 1999, and Aqua, launched 2002 [38]. The AVHRR (Advanced Very High Resolution Radiometer) is onboard the NOAA's (National Environmental Satellite, Data and Information Service) series of satellites and is like MODIS sensitive towards cloud cover [39].

The images from the different data sets are collected and studied after which the sea ice edge as well as the polygons of different ice concentration are manually drawn on the ice chart. The concentration is measured in tens, as discussed in section 3.4, and coloured according to the WMO international colour code, see figure 5.1b. The polygons are labelled with their respective properties, i.e. concentration, stage of development and form of ice, called Egg code due to the oval shape of the label (see figure 5.1a) [40]. WMO's Egg code, or international ice code, was introduced in 1982 and is still in use [41].

Colour		RGB colour model	Total concentration (definition from WMO Nomenclature)
alternative	prime		
		000-100-255	Ice free
		150-200-255	Less than one tenth (open water)
		140-255-160	1/10 - 3/10 (very open ice)
		255-255-000	4/10 - 6/10 (open ice)
		255-125-007	7/10 - 8/10 (close ice)
		255-000-000	9/10 - 10/10 (very close ice)
		150-150-150	Fast ice
		210-210-210	Ice shelf
	? ? ?	255-255-255	Undefined ice

Figure 5.1b. The standard WMO colour code for the different ice concentrations [40].

The ice charts at DMI are produced twice a week since 2010 before that they were made once a week, resulting in graphs that are slightly more detailed from 2010. Occasionally there is data missing which has been solved by taking the average value of the two adjacent dates.

The region chosen for this study is the east coast of Greenland, starting at the top of Fram Strait at 81ºN, all the way down and around the south tip at Cape Farvel, stretching down to 56ºN and 52ºW at the most. The area of interest is restricted to the west side of Svalbard at 10ºE and cutting diagonal through Greenland starting at 30ºW, to make sure all the fjords are accounted for. In this study the east coast of Greenland has been divided into three smaller areas, for a more regional analysis which can be seen in figure 1.2a. The first and north region is the one covering the Fram Strait and the northern part of the Greenland Sea, including the island of Jan Mayen. The second and central region is between 70ºN and 62ºN where the East Greenland shelf is somewhat altered, see figure 2.1a, and the water is deeper. The region covers the south part of the Greenland Sea and the Denmark Strait, between Greenland and Island. The south and final region reaches from 62ºN to 56ºN and covers the southern part of Greenland where weather conditions are rough and the ice cover is limited to the winter.

5.2. Passive microwave data - Northern Hemisphere

Passive microwave sensors on polar orbiting satellites are a very convenient way of monitoring the constricted and remote areas of the Northern Hemisphere, especially the inner Arctic. In this study sea ice extent data over the entire Northern Hemisphere has been achieved by DMI from satellites carrying passive microwave sensors, more specifically SSM/I (Special Sensor Microwave/Imager). The SSM/I sensors have a resolution of a couple of tens of kilometres, ranging from 12,5-30 km, and an unbroken data record since the launch of the first carrying satellite in 1981. SSM/I carrying satellites encircle the globe about 14 times a day giving a daily update on the sea ice extent, see figure 5.2a [3, 42].

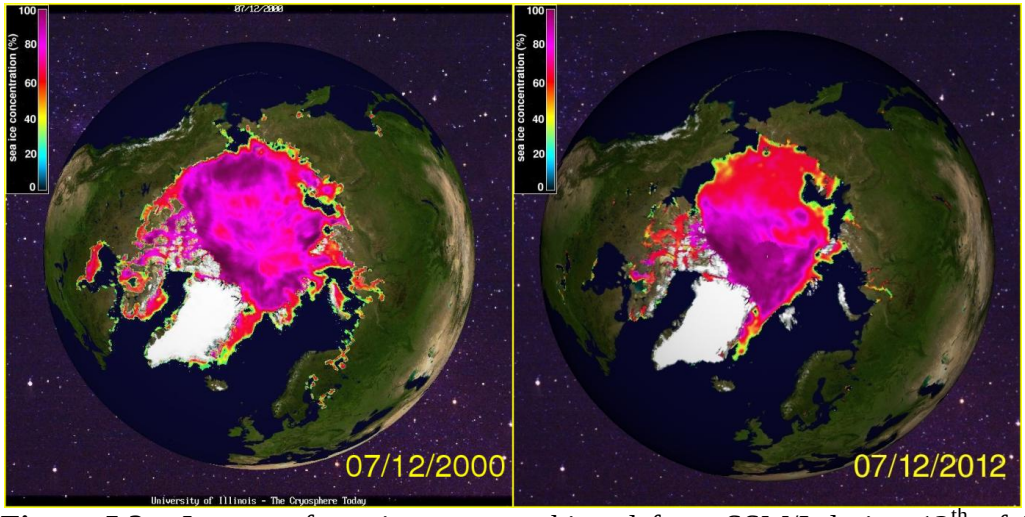

Figure 5.2a. Images of sea ice extent achieved from SSM/I during 12th of July 2000 and 2012, sea ice concentration of less than 30% is not displayed in these images [2].

The SSM/I data achieved for this study is from the Ocean and Sea Ice Satellite Application Facility-project (OSISAF), based in Norway, where ice concentrations over 30% are categorised as sea ice and the rest as open water [34]. The data for the present study is ranging from 2005-2012, due to technical difficulties the years 2000-2005 were inaccessible. The complete data set, stretching from 1978-present, was divided into two incomparable sets, one reanalysis stretching between the years 1978-2009 and the current measurement 2005-present [43]. In the current run an approximate, rather rough, coastline was inserted (see figure 5.2b) resulting in loss of data corresponding to a couple of millions of square kilometres, which makes the two sets impossible to put together. Additional missing data in both sets are due to lack of satellite coverage. The range 2005-2012 is however a good enough time interval to be able to spot a possible correlation between the ice extent in the entire Northern Hemisphere and the east coast of Greenland [13].

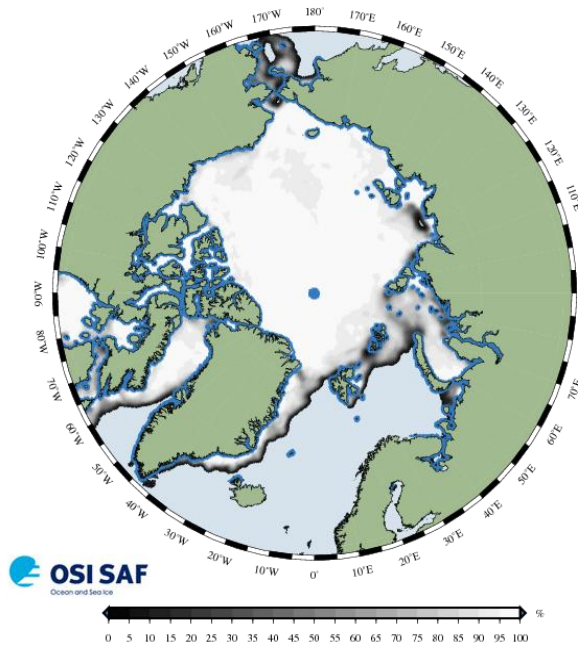

Figure 5.2b. Sea ice extent on the 23rd of May 2013, the blue line indicates the approximate coast line. [34]

SSM/I data is not as detailed as the produced ice charts, which in general has a higher ice concentration, but has a longer and more frequent record of measured data [15, 43]. Radars are a lot more precise than passive microwave satellites; they have a much higher resolution but a much smaller footprint and do not pass as often as the passive microwave satellites. Passive sensors are also a bit more sensitive towards water content in the atmosphere and melting of the sea ice, data of sea ice extent may have errors of several percent during the summer. The significant uncertainties regarding the position of the sea ice edge, especially during the summer, is why this study compares two different data sets. To be able to observe the variability of sea ice extent along the east coast of Greenland the accuracy has to be better than that of passive microwave sensors. There is a significant difference in the two ways of measuring the ice extent and an outright comparison might be foolish. However, in a relative comparison like this, over a long period of time, the differences are negligible [15, 44].

5.3. Pressure difference - The Fram Strait

A new method has been used to achieve the drift properties for the sea ice in the Fram Strait. By taking the pressure difference between two locations on either side of the strait it is possible to get an approximate strength and direction of the wind and thereby the ice drift in the Fram Strait [13]. Observation data has been collected from the weather stations Henrik Krøyer Holme (HKH) on Greenland and Ny Ålesund (NyÅ) on Svalbard between the years 2000-2012, see figure 5.3a. These two stations were chosen due to their position, almost in line on either side of Fram Strait, making it possible to get an approximation of the wind properties in the middle of the strait.

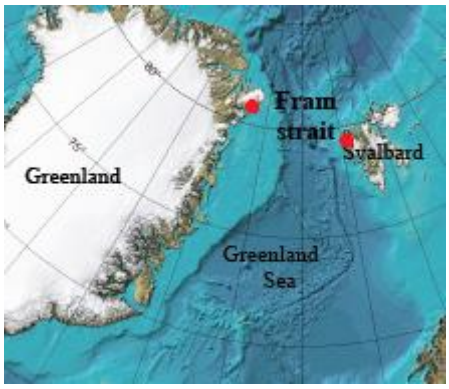

Figure 5.3a. The two weather stations on each side of the Fram Strait, as red dots, Henrik Krøyer Holme to the left on Greenland and Ny Ålesund to the right on Svalbard. The image is a part of the international bathymetric chart of the Arctic Ocean, modified by author [14].

The value received when taking the pressure (in hPa) at HKH and simply subtract the pressure at NyÅ may be either positive or negative and differ in size; a high positive value indicates strong northerly winds, transporting ice south out of Fram Strait, while a low and negative value indicates weak and southerly winds and a force driving the ice towards the north, see figure 5.3b. Comparisons between the pressure gradient and the variability of the sea ice have been done before, but to the author's knowledge it was never done using this method; approximate the wind direction and strength by calculating the pressure difference between two points on either side of the Fram Strait.

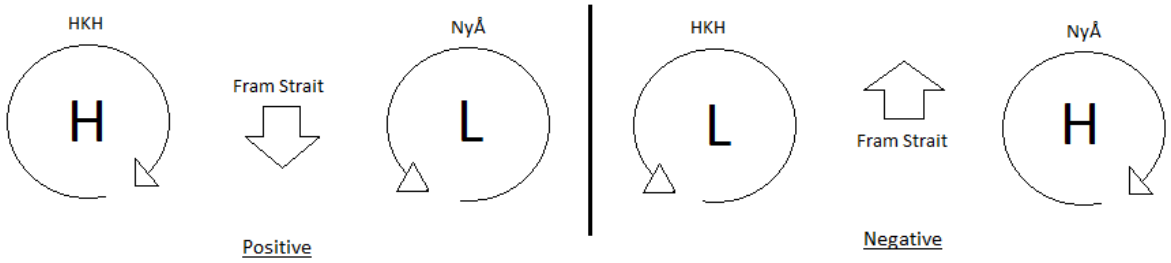

Figure 5.3b. Illustration of a situation with positive and negative pressure difference respectively, between HKH and NyÅ.

The pressure data received for this study contained big gaps which were impossible to fill in a relative easy and convenient way to be able to achieve values close to the actual data. However, where the gaps were small, i.e. 2-3 days, the slots were filled by taking the average value of the adjacent days.

6. Variability of Sea Ice Extent - Greenland

In this chapter the ice extent along the entire east coast of Greenland and the extent within three regional zones along the coast (see figure 1.2a), are compared with the variability of the whole Northern Hemisphere, for the years 2005-2012. The possibility of a correlation in the variability of the ice extents is examined and the cause of such a correlation/non-correlation is discussed. As described in chapter 5 two different sets of data are compared, the continuous passive microwave data for the entire Northern Hemisphere and the highly accurate sea ice charts over the east coast of Greenland.

The sea ice extent depends on the wind forcing which controls the ice drift and is due to pressure differences; thus the ice extent is expected to be highly correlated with the pressure difference. In this study a comparison is made, during the period 2000-2012, between the ice extent along the east coast of Greenland and the pressure difference between the two sides of Fram Strait, i.e. the weather stations Henrik Krøyer Holme (HKH) on Greenland and Ny Ålesund (NyÅ) on Svalbard, see figure 5.3a. The east coast is further divided into three parts to study variations in the correlation strength as well as the possibility of a time delay between the different regions and the effect of the pressure difference across the strait.

6.1. The east coast of Greenland and the Northern Hemisphere

In this study the variability of the sea ice extent is analysed during the period 2005-2012, by the use of data from satellite remote sensing, both direct images and manually created ice charts.

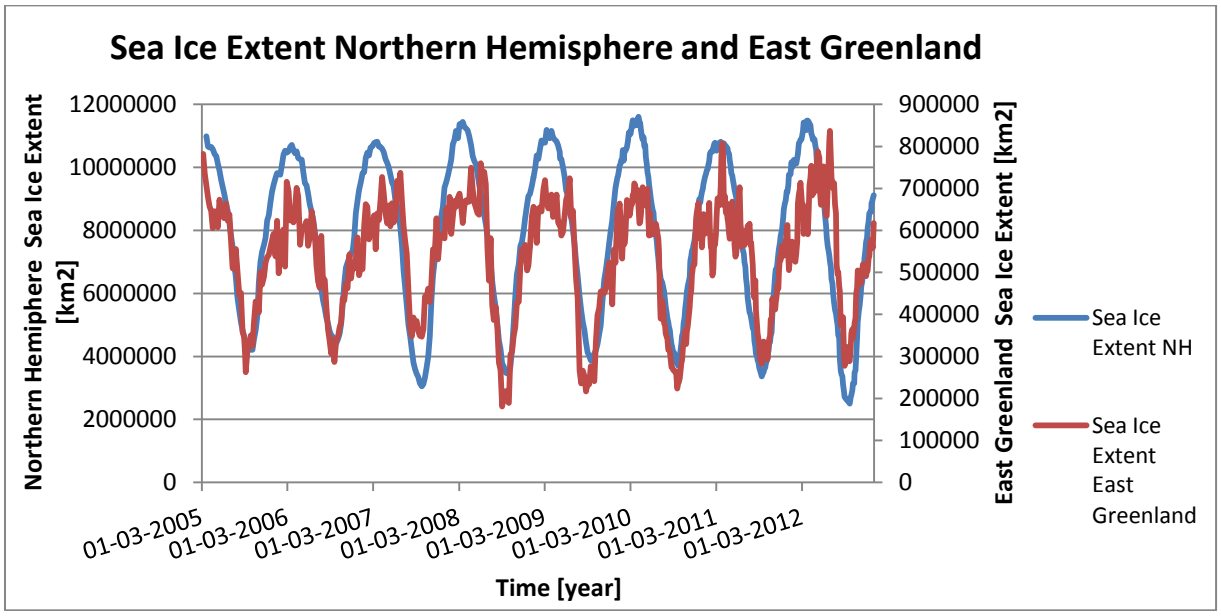

Figure 6.1a. The sea ice extent in the entire Northern Hemisphere (blue line) and along the east coast of Greenland (red line). Measurments starting on the 6th of March 2005 ending on the 30th of December 2012, once a week until 2010 then twice a week.

In figure 6.1a the annual variation of the sea ice extent in the Northern Hemisphere and in the region along the east coast of Greenland is clearly visible, with the annual maximum in March and the annual minimum in September. The extremes are smother and clearer in the Northern

Hemisphere then in the east coast of Greenland and roughly of an order of magnitude larger. From the figure it is apparent that the variations of the annual minimum extent are much more significant than the maximum. During the period 2005-2012 the maximum ice extent in the Northern Hemisphere has an average of 11,0 million square kilomtres with an absolute maximum in 2010 of 11,6 million square kilometres. The east coast of Greenland has a maximum average of 676'000 km^2 with the larget ice extent in 2011 and in June 2012, of 807'000 and 837'000 respectively.

The average minimum ice extent of the Northern Hemisphere is 3,8 million square kilometres with the lowest value of 2,7 million square kilometres in 2012, and the second lowest in 2007 coinciding with the highest minimum value for the east coast of Greenland. The average minimum value for the east coast of Greenland is 287'000 km^2, with the highest value in 2007 and the lowest in the following year (2008), see figure 6.1b. The expectations were to see more situations of negative correlation between the two regions such as the minimum extent in 2007. Due to the fact that a decreased ice extent in the Arctic leads to an increase in the sea ice mobility, thus more ice may be transported through the Fram Strait. However the magnitude of the Greenland sea ice extent seems unaffected by the expected affects of the decrease in Arctic. The decrease of the sea ice extent in the Arctic region is mainly in the most remote areas, relative Fram Strait, such as the Beaufort and Chukchi Sea which can be seen in figure 6.1b. The sea ice decrease in those areas does not significantly affect the inflow to the Fram Strait, which could explain the lack of negativly correlated events.

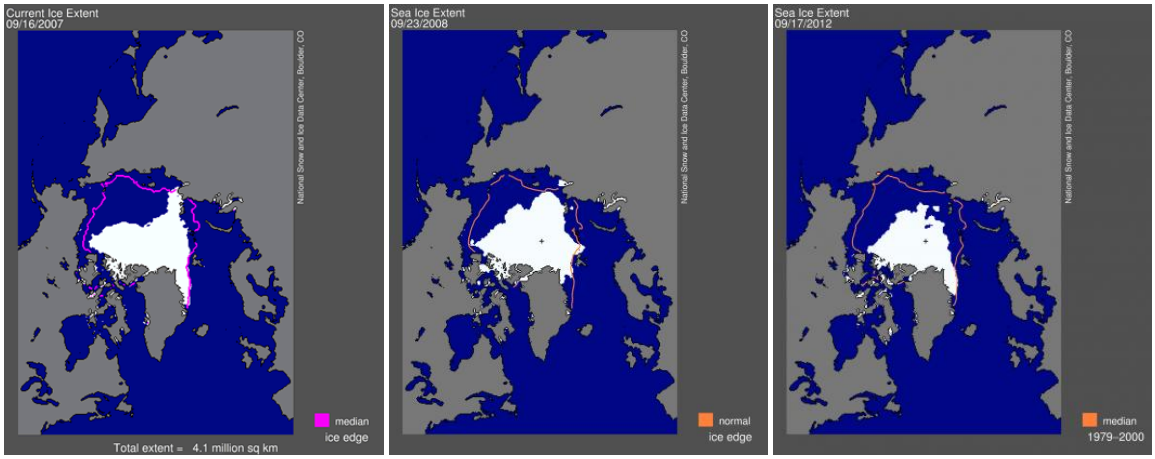

Figure 6.1b. The minimum ice extent in the Northern Hemisphere 2007, 2008 and 2012 respectively. The purple and orange lines show the 1979 to 2000 median ice edge [30].

To be able to better observe and compare the variability of the ice extent between the two areas it is convenient to focus on the extremes and solely compare annual maxima and minima, see figure 6.1c and 6.1d. There seems to be a better correlation between the maximum values than between the minimum values, which could be due to the impact of large weather systems. During winter when the pressure patterns are more distinct they may affect vast areas in a similar way resulting in a possible correlation between the entire Hemisphere and the east coast of Greenland. During summer the weather systems entering the region are much weaker and only affect regional areas, thus the east coast of Greenland may be experiencing completely different conditions relative the adjacent Barents Sea or the central Arctic Ocean for instance.

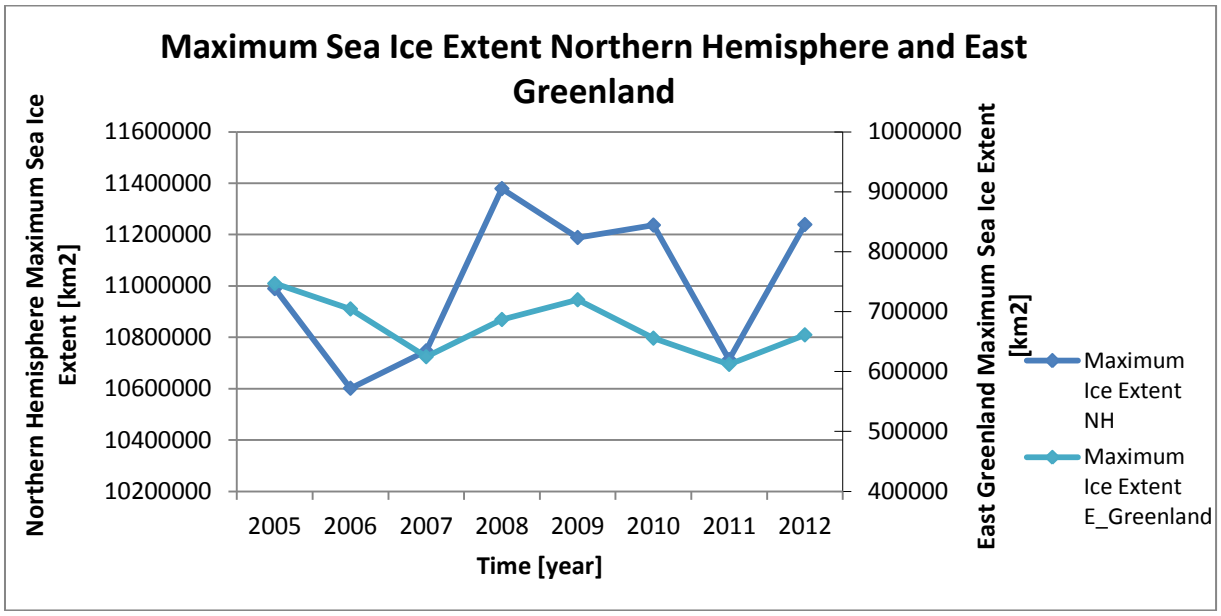

Figure 6.1c. The annual sea ice maximum in March in the Northern Hemisphere as well as along the east coast of Greenland, 2005-2012.

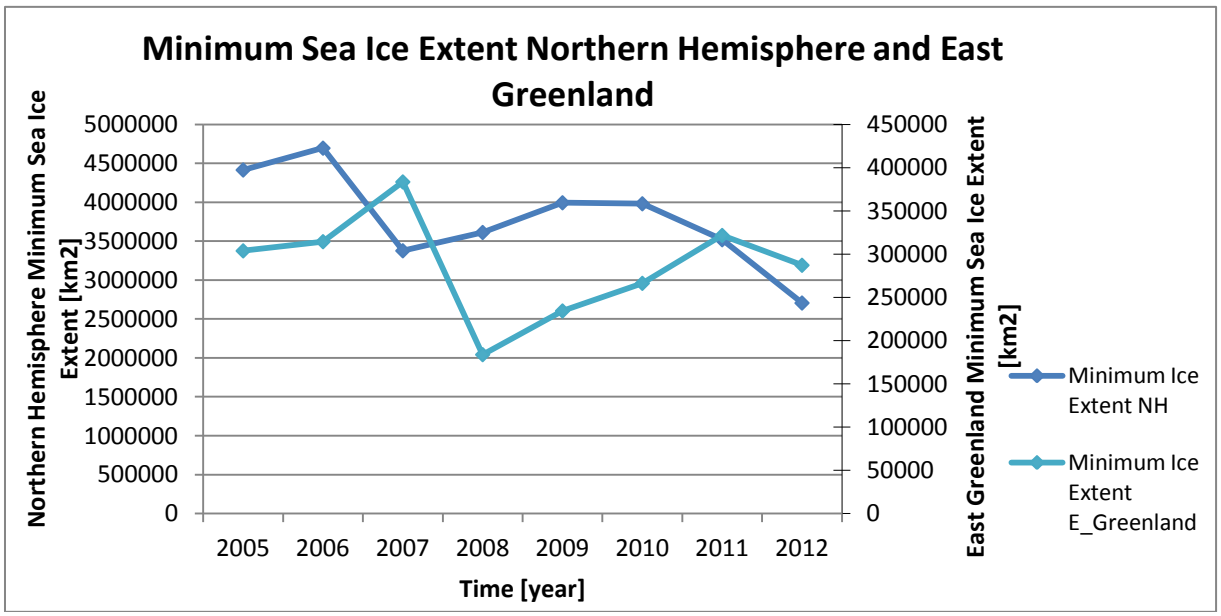

Figure 6.1d. The annual sea ice minimum in September in the Northern Hemisphere as well as along the east coast of Greenland, 2005-2012.

The perception that the maximum values correlate better than the minimum values is consistent when calculating the sea ice anomalies from the annual extreme values, see figure 6.1e and 6.1f. The maximum anomaly graph has indeed a higher correlation with a coefficient of determination (R-squared) approximately equals 0,06 while the minimum anomaly graph only has an R-squared of 0,00. However the correlations are not significant, indicating that there is not a relation between the sea ice extent in the Northern Hemisphere and along the east coast of Greenland.

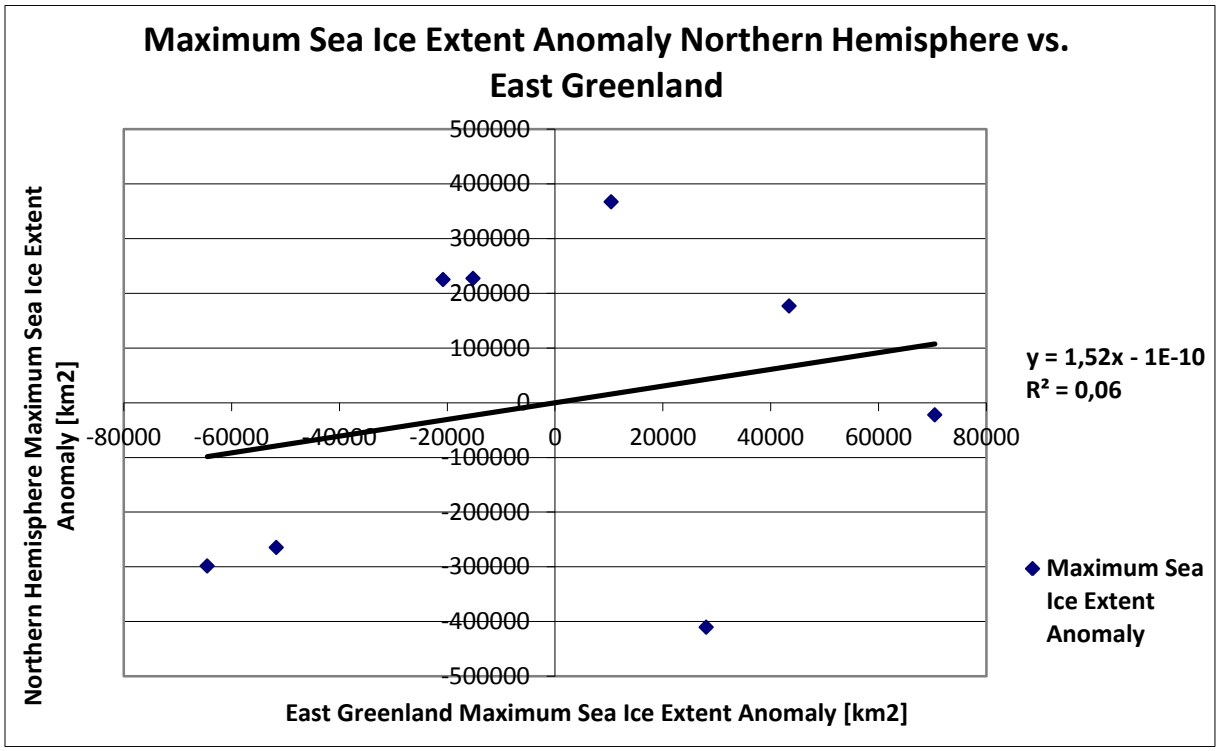

Figure 6.1e. The annual maximum sea ice extent anomalies for the Northern Hemisphere versus the east coast of Greenland, calculated from the annual maximum extent (2005-2012) 11,0 million square kilomtres for the Northern Hemisphere and 676'000 for the East Greenland.

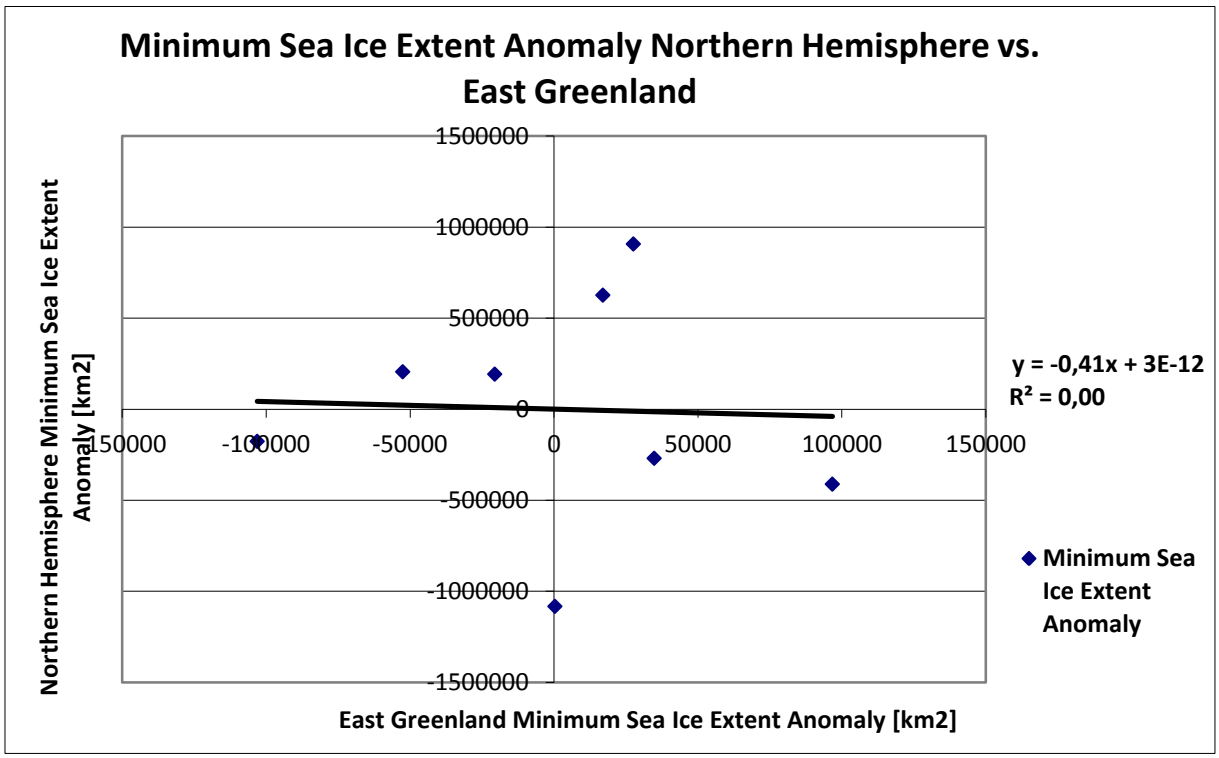

Figure 6.1f. The annual minimum sea ice extent anomalies for the Northern Hemisphere versus the east coast of Greenland, calculated from the annual minimum extent (2005-2012) 3,8 million square kilometres for the Northern Hemisphere and 287'000 km^2 for the East Greenland.

The non-correlation displayed in figure 6.1e and 6.1f depends on a range of factors, but above all on the size difference of the two compared regions, one being half the globe and the other one just about 2000*1000 km^2. The size difference implies that the regions are affected by very different atmospheric and oceanic forces, even though East Greenland is a part of the Northern Hemisphere there is a lot of parameters to take into account when comparing the two regions. For instance there are not too many places in the Arctic where the ice is able to grow and expand; during the winter the major ice growth occurs in the Bering Strait, Baffin Bay as well as the Barents and Greenland Seas. The last two regions may experience similar conditions but may as well be equalized by a remote area such as the Bering Strait. Thus the rate of new ice formation in the Greenland Sea, almost completely cut off from the central Arctic region, may significantly alter the variability of the sea ice extent along the east coast of Greenland.

	Maximum		**Minimum**	
Northern Hemisphere Sea Ice Extent Anomaly vs.:	**Linear Equation**	**R^2**	**Linear Equation**	**R^2**
North 81N_70N Sea Ice Extent Anomaly	$IE_N = 0{,}00IE_{NH}$	0,00	$IE_N = -0{,}01IE_{NH}$ -1E-11	0,02
Central 70N_65N Sea Ice Extent Anomaly	$IE_C = -0{,}00IE_{NH}$	0,00	$IE_C = 0{,}01IE_{NH}$ - 5E-13	0,19
South 65N_56N Sea Ice Extent Anomaly	$IE_S = 0{,}04IE_{NH}$-4E-12	0,22	$IE_S = 0{,}00IE_{NH}$ - 9E-14	0,28

Table 6.1. The sea ice extent anomalies for the annual maximum and minimum periods in the Northern Hemisphere (IE_{NH}) are compared with the corresponding sea ice extent anomalies in the 3 zones along the east coast of Greenland ($IE_{N,C \text{ and } S}$). The linear equations and the R-squared from the respective plots (not displayed here) are stated above, with two significant digits.

In table 6.1 the results from the comparison between the maximum and minimum sea ice extent anomalies in the Northern Hemisphere and the 3 zones along the east coast of Greenland are summarized. In contrary to the result for the entire east coast the R-squared values indicate a higher correlation between the minimum values. This may be due to the lack of new ice formation during the summer, thus the ice extent is solely dependent on various ice drift and deformation parameters which may have a more equal affect throughout the Northern Hemisphere. The results in table 6.1 displays a significant difference between the correlation of the anomalies for the different zones, with the northern zone displaying a clear non-correlation and the southern a rather high correlation to the anomalies in the Northern Hemisphere. What this correlation difference depends on is uncertain and requires further studies. However it seems as if the southern part of the east coast is experiencing somewhat the same forcing as the entire Arctic area, while the northern and central parts are affected by more regional conditions. It is possible that the drift through Fram Strait affects the two northernmost regions more than the south and that is a likely reason why they are less correlated to the ice extent in the entire Northern Hemisphere.

6.2. The East coast of Greenland and the pressure difference

In this section a comparison is made, during the period 2000-2012, between the ice extent along the east coast of Greenland and the pressure difference between the two sides of Fram Strait, i.e. the weather stations Henrik Krøyer Holme (HKH) and Ny Ålesund (NyÅ), see figure 5.3a. The east coast is further divided into three parts to examine variations in the correlation strength as well as the possibility of a time delay between the different regions and the effect of the pressure difference across the strait.

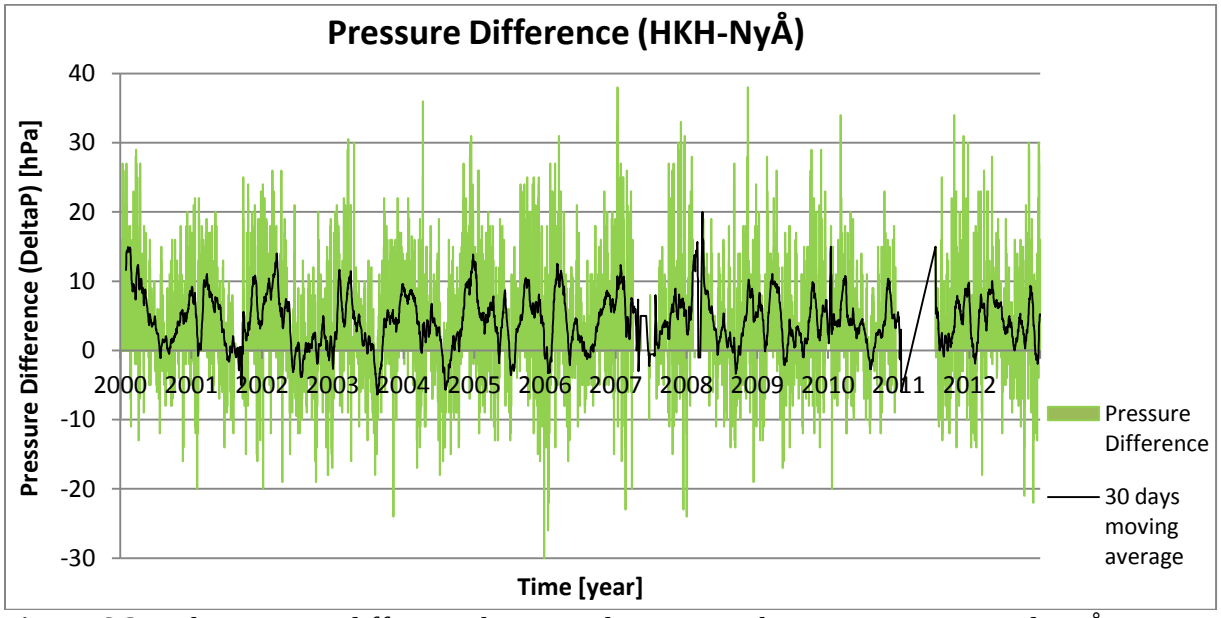

Figure 6.2a. The pressure difference between the two weather stations HKH and NyÅ on either side of the Fram Strait, during the period 2000-2012. The black curve displays a 30 days moving average.

The pressure difference between the two weather stations displayed in figure 6.2a shows a dominant positive pressure difference, i.e. northerly winds and an ice drift down south through Fram Strait. The year of 2008 stands out as a year of especially high positive drift which should be reflected in an increase of the sea ice extent along the east coast of Greenland, i.e. if there is a correlation. Periods of low pressure difference and low southward drifts as the years 2004 and the beginning of 2006 ought to be reflected as years of low sea ice extent along the coast.

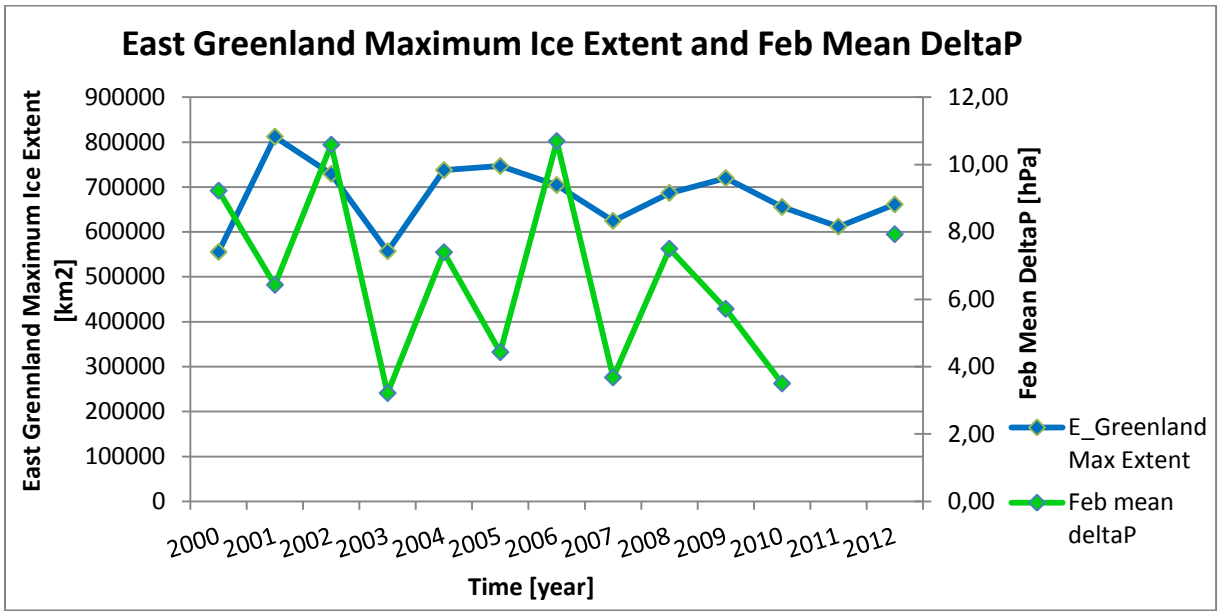

Figure 6.2b. The annual maximum sea ice extent in March along the entire east coast of Greenland, 2000-2012, and the mean pressure difference (deltaP) during the previous month, i.e. February. The data for the year 2011 are missing due to an incomplete data set.

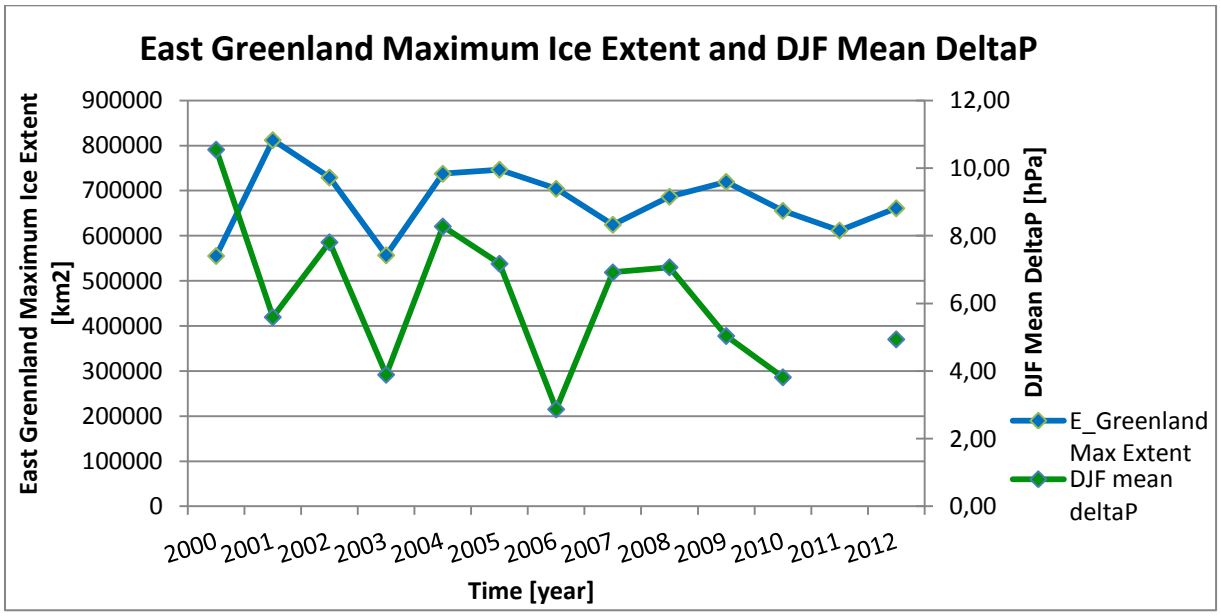

Figure 6.2c. The annual maximum ice extent along the east coast of Greenland and the pressure difference averaged over the previous three months, December-February.

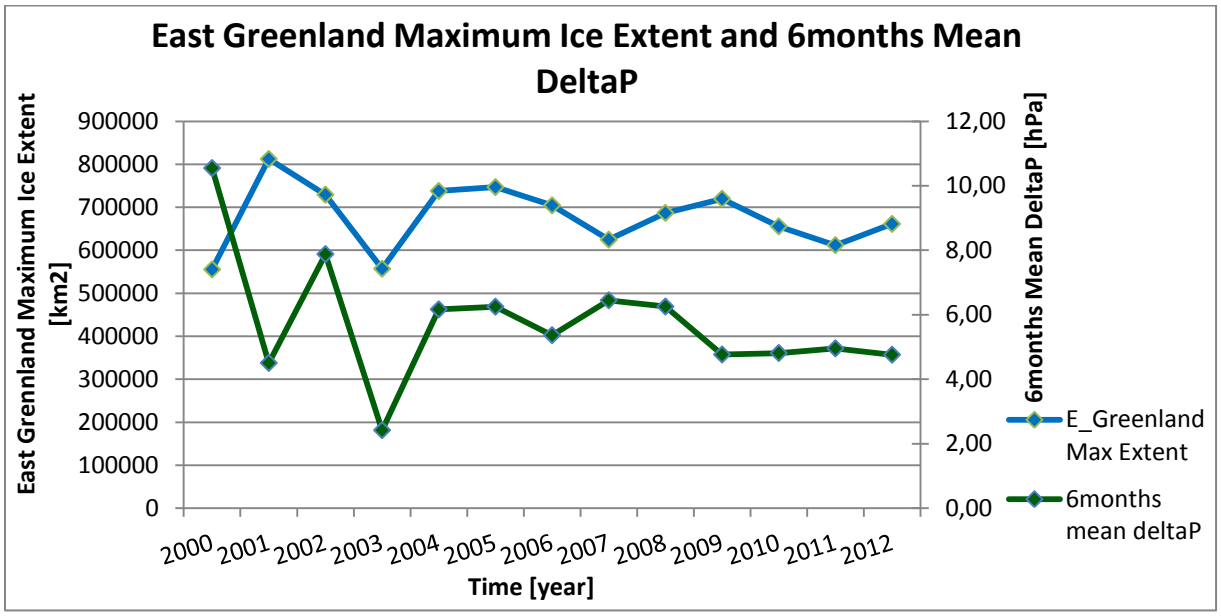

Figure 6.2d. The maximum sea ice extent along the east coast of Greenland and the pressure difference averaged over the previous six months, September-February.

According to the figures 6.2b-d there appears to be a correlation between the maximum value of the ice extent in the area along the east coast of Greenland and the pressure difference, and it seems as if the correlation gets stronger with increasing time intervals. There is however a stronger correlation between the minimum ice extent and the pressure difference, according to the figures 6.2e-g. The stronger correlation could be explained by the lack of new ice formation during the summer. In the summer months the ice melts and there is no new ice formation, thus the ice extent is significantly dependent on the ice drift, and secondary on the temperature controlling the rate of the ice melt. That is in contrast to the winter months when the ice extent depends more equally on the drift and the surface temperature which then controls the rate of new ice formation.

In the figures 6.2e-g the correlation seems to be strongest for the shorter periods of time reflecting the fact that the sea ice extent minimum, which occurs during the summer, is more sensitive towards the weather conditions and due to the lack of new ice formation responds to pressure changes much faster.

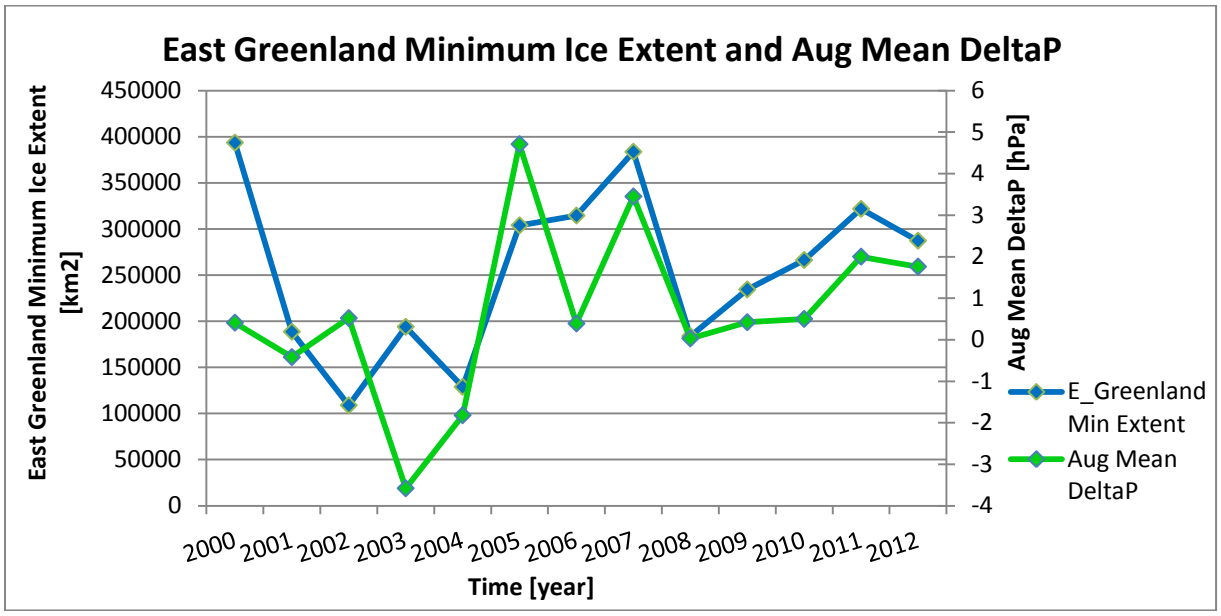

Figure 6.2e. The annual minimum sea ice extent in September along the east cost of Greenland and the mean pressure difference in August.

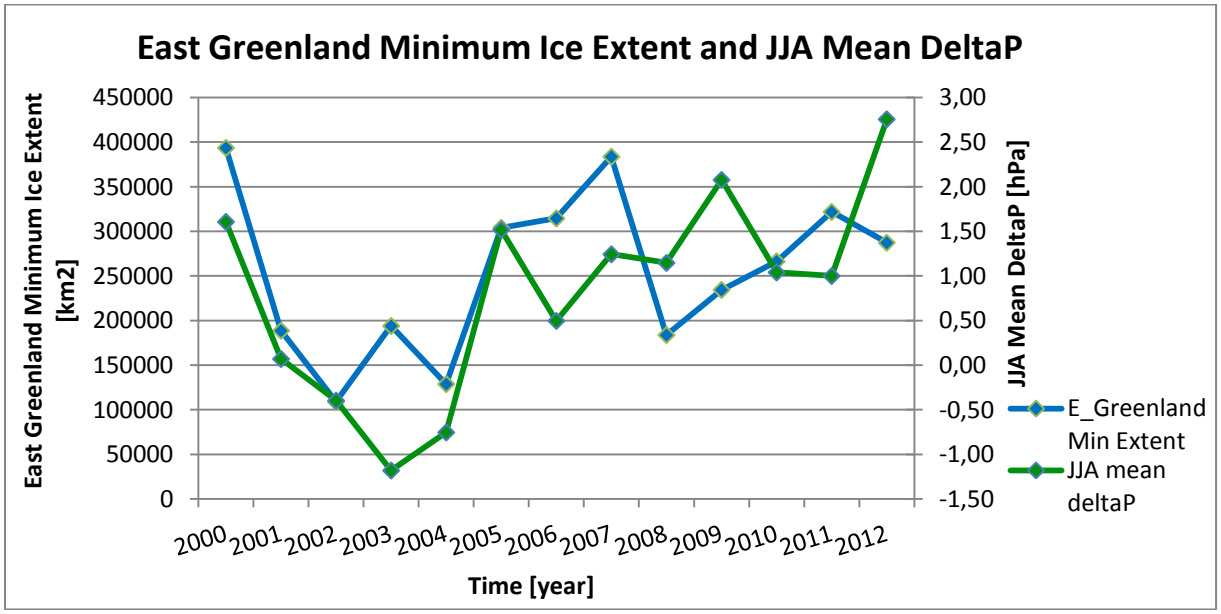

Figure 6.2f. The annual minimum sea ice extent along the east coast of Greenland and the pressure difference averaged over the three previous months, June-August.

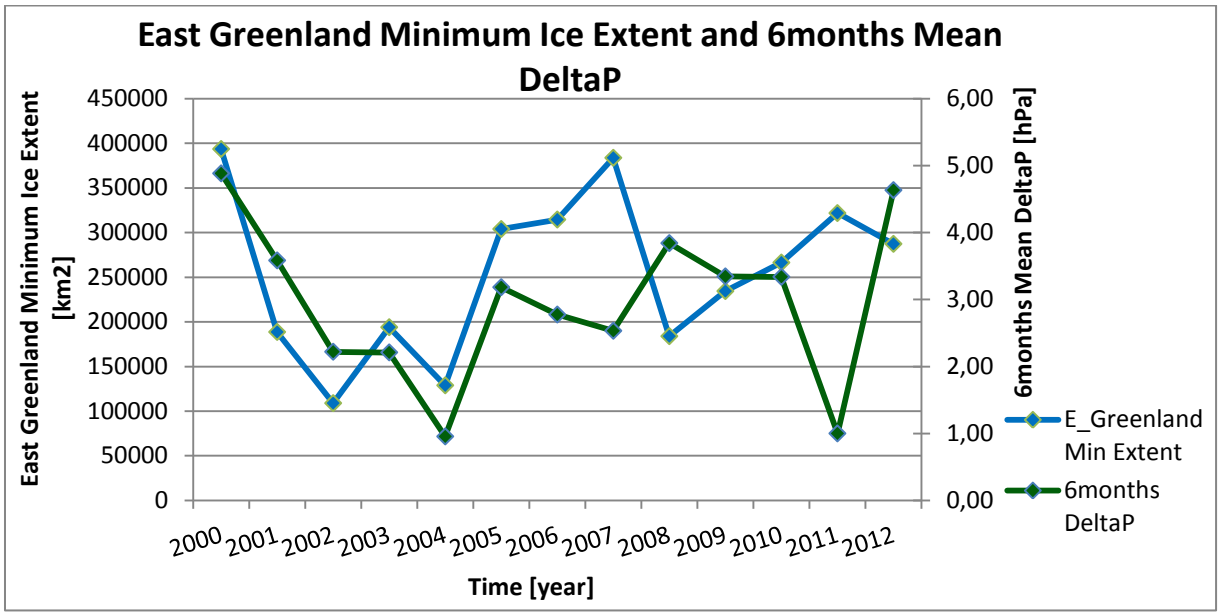

Figure 6.2g. The annual minimum sea ice extent along the east coast of Greenland and the mean pressure difference for the six previous months, March-August.

In this study a linear dependence between the sea ice extent along the east coast of Greenland and the pressure difference across the Fram Strait is sought, i.e. $IE_G = f(\Delta P)$. Where the ice extent along the east coast of Greenland (IE_G) depends solely on the pressure difference (ΔP). It is noted however, that the dependence is more complex than that. To get a better correlation to the ice extent more parameters must be accounted for.

The conceptual model in figure 6.2h illustrates the two main factors affecting the ice extent along the east coast of Greenland, the pressure difference across the Fram Strait and the surface air temperature. The two parameters are coupled in a relation for the sea ice extent (IE_G) depending on both the pressure difference (ΔP) and the temperature (T), $IE_G = f(\Delta P, T)$. In the case where the pressure difference between Greenland and Svalbard are positive (situation 1. in figure 6.2h) there is a southward transport through the Fram Strait and thereby a positive ice drift. The temperature has different rates of affect during the winter and the summer; in the winter situation (2.) a positive temperature anomaly along with a positive sea ice drift (5.) results in a neutral ice extent (see table 6.2a) as the two forces cancel each other. A positive temperature anomaly results in a reduced new ice formation, while a negative temperature anomaly as in situation 4 results in significant new ice formation. Situation 4 results in a very high ice extent in the area with both new ice formation and positive drift. During the summer the situation is somewhat different; a negative temperature anomaly along with a positive drift, as in situation 6, results in a very high ice extent predominantly due to the drift and secondary due to the low rate of melting. However a positive temperature anomaly during the summer along with the positive drift situation (7.) will still result in a high ice extent. Due to the drift, which is the major factor during the summer the ice extent will be above neutral in both situation 6 and 7 in figure 6.2h.

If the drift situation is negative, as situation -1 in figure 6.2h, the ice extent will be lower than during a positive drift period, predominantly during the summer. A winter situation with both negative drift and temperature anomalies, like situation -4, results in a neutral ice extent. A situation with a positive temperature anomaly on the other hand results in a very low ice

extent, where there is reduced new ice formation and a northward transport of the ice. A negative drift situation during the summer with negative temperature anomaly (-6.) results in a low ice extent, where the rate of ice melt is relative low. However, positive temperature anomalies, as situation -7, result in a very low ice extent where there is no transport of new ice to the area and a high rate of melting.

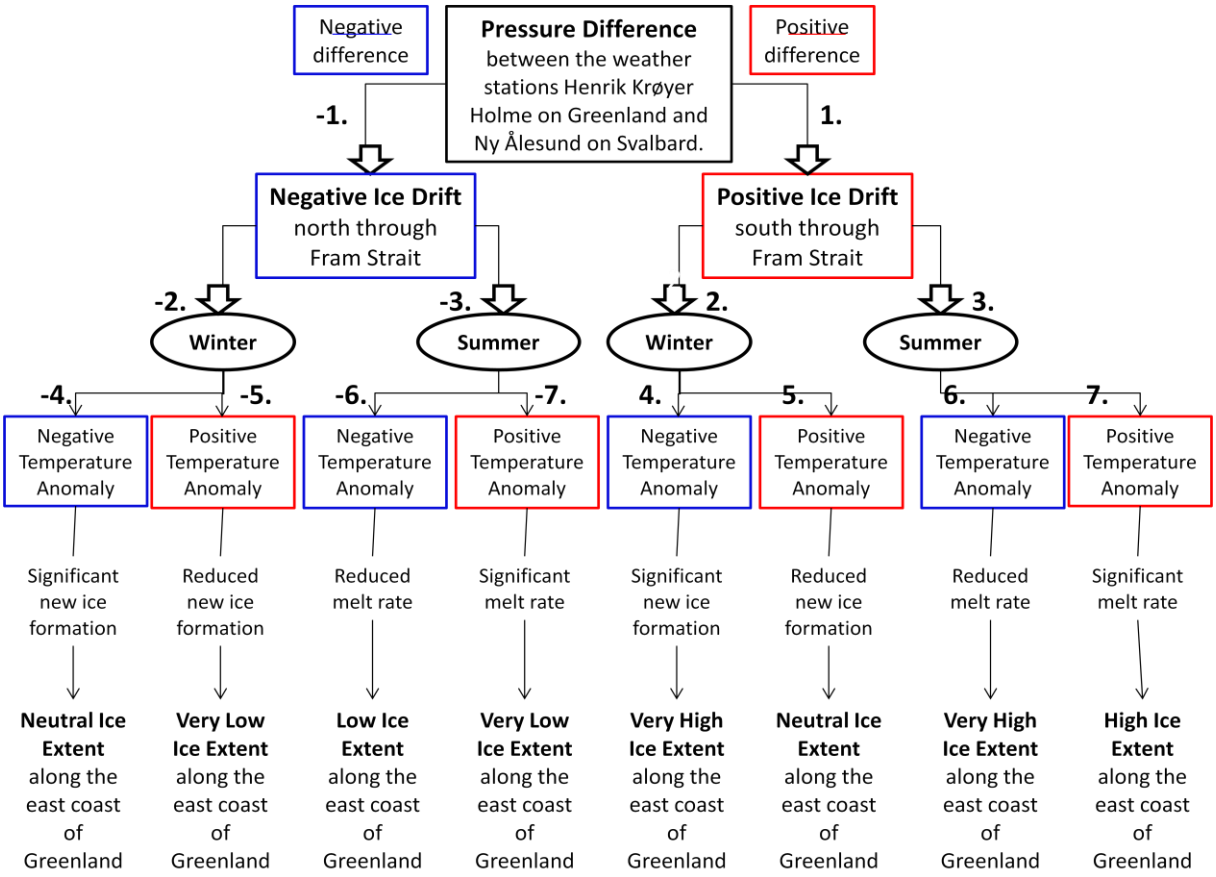

Figure 6.2h. Conceptual model of the two major parameters affecting the sea ice extent along the east coast of Greenland, pressure difference and temperature, $IE_G = f(\Delta P, T)$. The temperature is a secondary parameter during the summer period. The values, for the east coast of Greenland, corresponding to the expressions very high sea ice extent, high, neutral, low and very low are defined in table 6.2a below.

Sea Ice Extent Along the East Coast of Greenland	Maximum [km^2]	Minimum [km^2]
Very High	800 000	400 000
High	740 000	345 000
Neutral	680 000	290 000
Low	615 000	200 000
Very Low	550 000	110 000

Table 6.2a. The values for the east coast of Greenland, 2000-2012, corresponding to the expressions very high sea ice extent, high, neutral, low and very low used in figure 6.2h. The neutral values are the average values for the period 2000-2012 and the very high and very low values are the extreme values from the figures 6.2b-g.

6.2.1. Sea ice extent anomalies versus pressure difference anomalies

The annual maximum and minimum sea ice extent anomalies has been derived and plotted against the mean pressure difference anomalies calculated for the previous month, three months and six months. The result of the comparisons are all summarized in table 6.2.1a and 6.2.1b, in the tables are also presented the results from the three regional zones along the east coast of Greenland.

MAXIMUM	**Time interval**		
Area	1 month mean deltaP February	3 months mean deltaP Dec-Feb	6 months mean deltaP Sep-Feb
All East Greenland	$IE_G = 7400\Delta P + 3800$ $R^2 = 0,09$	$IE_G = 2800\Delta P + 1300$ $R^2 = 0,01$	$IE_G = -5400\Delta P + 1E-10$ $R^2 = 0,02$
North 81N_70N	$IE_N = 1800\Delta P + 930$ $R^2 = 0,01$	$IE_N = -2100\Delta P - 994,86$ $R^2 = 0,01$	$IE_N = -16000\Delta P+3E-11$ $R^2 = 0,20$
Central 70N_65N	$IE_C = 5100\Delta P + 2600$ $R^2 = 0,17$	$IE_C = 6100\Delta P + 2900$ $R^2 = 0,18$	$IE_C = 9400\Delta P - 2E-11$ $R^2 = 0,20$
South 65N_56N	$IE_S = 280\Delta P + 150$ $R^2 = 0,02$	$IE_S = -1300\Delta P - 620$ $R^2 = 0,03$	$IE_S = 1200\Delta P - 6E-12$ $R^2 = 0,01$

Table 6.2.1a. The maximum sea ice extent anomalies along the entire east coast of Greenland (IE_G) and in the three zones ($IE_{N,C \text{ and } S}$) against the mean pressure difference anomalies (ΔP) calculated over three different time intervals. The linear equations as well as the R-squared values are displayed in the table with two significant digits.

MINIMUM	**Time interval**		
Area	1 month mean deltaP August	3 months mean deltaP June-Aug	6 months mean deltaP March-Aug
All East Greenland	$IE_G = 25000\Delta P-3E-11$ $R^2 = 0,35$	$IE_G = 49000\Delta P - 3E-11$ $R^2 = 0,38$	$IE_G = 25000\Delta P - 4E-11$ $R^2 = 0,11$
North 81N_70N	$IE_N =22000\Delta P+4E-11$ $R^2 = 0,29$	$IE_N = 47000\Delta P + 4E-11$ $R^2 = 0,38$	$IE_N = 26000\Delta P + 3E-11$ $R^2 = 0,13$
Central 70N_65N	$IE_C = 2500\Delta P - 5E-14$ $R^2 = 0,37$	$IE_C = 1300\Delta P + 4E-13$ $R^2 = 0,03$	$IE_C = -1,3\Delta P + 4E-13$ $R^2 = 0,00$
South 65N_56N	$IE_S = 600\Delta P - 2E-13$ $R^2 = 0,20$	$IE_S = 440\Delta P - 5E-14$ $R^2 = 0,03$	$IE_S = -380\Delta P + 8E-14$ $R^2 = 0,03$

Table 6.2.1b. The minimum sea ice extent anomalies along the entire east coast of Greenland (IE_G) and in the three zones ($IE_{N,C \text{ and } S}$) against the mean pressure difference anomalies (ΔP) calculated over three different time intervals. The linear equations as well as the R-squared values are displayed in the table with two significant digits.

For the maximum sea ice extent anomalies along the entire east coast, see table 6.2.1a, the correlation seems to be better for the shortest time interval while the north and central zones have an increasing correlation towards the higher interval. The south zone however has best response to the mean pressure difference anomalies calculated over three months. This contradicts the expectations that the correlation for the northerly zone would be most significant for a pressure difference calculated over a short period and the southerly zone for a

long period, due to the time it takes for the ice to get transported down along the coast of Greenland.

It may not be quite correct to talk about a correlation between the maximum sea ice extent anomalies and the pressure difference anomalies as the connections in general are quite small, especially in comparison to the minimum. In table 6.2.1b there is an apparent correlation between the anomalies for the annual minimum sea ice extent and the mean pressure difference across the Fram Strait. The extent along the entire coast and in the north zone are best correlated with the three-months mean, while the central and south zones are best fitted to the one-month mean after which it subsides. It is possible that the correlation for the northernmost region had been even better if the pressure would be calculated over a two-month period. However, there is also a clear trend of decreasing correlation down through the three zones. The north zone is most correlated to the mean pressure difference, which is expected as the pressure difference is calculated within the north zone and ought to have most significant affect there.

It is clear from the tables 6.2.1a and 6.2.1b that there is a connection between the pressure difference across the Fram Strait and the ice extent in the area. The pressure difference explains up to one third of the variations in the extent, with a stronger correlation during the summer. The remaining two thirds may be explained by a combination of other parameters, but predominantly by the air temperature which controls the rate of new ice formation during the winter and the rate of sea ice melt during the summer. As explained in figure 6.2h the two parameters interact differently throughout the year, additional contribution to the variability of the sea ice extent may come from the sea surface temperature and changes in big scale pressure systems. The Arctic Oscillation and North Atlantic Oscillations have just briefly been compared to the different years of ice extent during this work, but no conclusions could be drawn.

It is concluded that there is a correlation between ice extent along the east coast of Greenland and the pressure difference across Fram Strait. The sea ice extent maximum, during the winter, has a stronger dependence tentatively on the temperature, which controls the rate of new ice formation. As mentioned earlier in this section, there is no new ice formation during the summer and the sea ice extent has a higher dependence on the ice drift and thereby on the pressure difference across the Fram Strait. In this study a very simple model has been analysed with only the pressure difference as a parameter, a linear relation, for a better connection with the ice extent the air temperature should be accounted for. The pressure difference and the temperature are interdependent and may enhance or counteract each other as illustrated in figure 6.2h. In the summer the temperature is a secondary parameter and during the winter it may be the dominant factor of the ice extent. How big the dependence is would be an interesting subject for further studies.

7. Conclusion

This bachelor thesis has examined the variability of the sea ice extent along the east coast of Greenland.

Data from manually produced ice charts over the east coast of Greenland have been compared with passive microwave data of the entire Northern Hemisphere, for the years 2005-2012, to find a possible correlation between the sea ice extents. The expectations were to observe a negative correlation, if any, between the two regions due to the fact that a decreased ice extent in the Arctic leads to an increase in the sea ice mobility [10]. Thus more ice may be transported through the Fram Strait, resulting in an increase of the sea ice extent along the east coast of Greenland coinciding with a decrease in the whole Northern Hemisphere. However the decrease of the sea ice extent in the Arctic region is mainly in the most remote areas relative the Fram Strait, and the results presented in this study shows an unaffected ice drift through the strait. The figures 6.1e and 6.1f showed a non-correlation between the ice extent along the east coast of Greenland and the ice extent in the entire Northern Hemisphere. The R-squared values for the annual sea ice maximum and minimum respectively were 0,06 and 0,00.

The non-correlation between the sea ice extents in the entire Northern Hemisphere relative the east coast of Greenland, displayed in figure 6.1e and 6.1f, is expected to depend on many things but predominantly on the size difference of the two compared regions. The significant size difference implies that the regions are affected by very different atmospheric and oceanic forces and there are a significant number of parameters to take into account when comparing the two regions. However when comparing the ice extent of three smaller regions along the east coast of Greenland, see figure 1.2a, with the extent in the entire Northern Hemisphere there was in fact a correlation for the two most southward regions, especially for the annual minimum ice extent values displayed in table 6.1. The higher correlation for the minimum extents may be due to the lack of new ice formation during the summer, thus the ice extent is solely dependent on various ice drift and deformation parameters which may have a more equal affect throughout the Northern Hemisphere.

In this study the ice extent along the east coast of Greenland has also been compared with the pressure difference across the Fram Strait, during the years 2000-2012. A special method has been used to achieve the drift properties for the sea ice in the Fram Strait [13]. By taking the pressure difference between two weather stations on either side of the strait, i.e. Henrik Krøyer Holme on Greenland and Ny Ålesund on Svalbard it was possible to get an approximate strength and direction of the wind and thereby of the ice drift in the middle of the Fram Strait. The maximum and minimum sea ice extent values for the entire east coast of Greenland and for three regional zones along the coast were compared with the mean pressure difference calculated for three different periods: the previous one month, three months and six months respectively.

There was a correlation between the sea ice extent in the different regions along the east coast of Greenland and the mean pressure difference. The expected time delay between the mean pressure difference and the ice extent in the three zones along the coast, due to the transport of the ice, was contradicted by the results in table 6.2.1a and 6.2.1b. The maximum sea ice extent anomalies for the north and central zones had an increasing correlation towards the

higher time intervals while the south zone had best response to the mean pressure difference anomalies calculated over the shorter three-month period. The annual minimum sea ice extent anomalies for the north zone were best correlated with the three-month mean, while the central and south zones were best fitted to the one-month mean after which it subsided. It is possible that the correlation for the northernmost region had been even better if the pressure would have been calculated over a two-month period.

The results in table 6.2.1b displayed a clear trend of decreasing correlation down through the three zones with the northerly zone most correlated to the pressure difference. The results were expected as the pressure difference was calculated across the Fram Strait which is located within the northern region, thus the affect on the ice ought to be most significant in that region.

The correlation was more significant for the annual minimum than for the annual maximum sea ice extent, which had several R-squared values around 0,3. The correlation for the maximum values seemed to increase for the longer periods of calculated pressure difference while the correlation for the minimum values seemed to increase for the shorter periods. This reflects the fact that the sea ice extent minimum, which occurs during the summer, is more sensitive towards the weather conditions and due to the lack of new ice formation responds to pressure changes much faster. In the summer months the ice melts and there is no new ice formation, thus the ice extent is predominantly dependent on the ice drift and secondary on the temperature controlling the rate of the ice melt as displayed in the conceptual model in figure 6.2h. This may explain why the sea ice extent values for the annual minimum extent had a more significant correlation to the pressure difference than the annual maximum extent.

In this study a linear dependence between the sea ice extent along the east coast of Greenland and the pressure difference across the Fram Strait was sought. It is concluded however, that the dependence is more complex than that. The pressure difference alone does not fully predict the variability of the sea ice extent along the east coast of Greenland, it explains about one third. To better be able to predict the variability of the sea ice extent the air temperature should be accounted for. The pressure difference and the temperature are interdependent and may enhance or counteract each other as illustrated in figure 6.2h. In the summer the temperature is a secondary parameter and during the winter it may be the dominant factor of the ice extent. Other parameters that may affect the variability of the sea ice extent are variations in the big atmospheric oscillations such as the AO and NAO, ocean currents and the sea surface temperature.

This study has showed the ice extent along the east coast of Greenland to be non-correlated with the ice extent in the entire Northern Hemisphere and dependent on the pressure difference across the Fram Strait, especially during the summer months. There is however an unknown uncertainty in the correlation which may be subject for further studies. To be able to establish a long-term correlation between the sea ice extent along the east coast of Greenland and the pressure difference across the Fram Strait, and reduce the uncertainties, a comparison of an extended time interval would be of interest for further studies.

Acknowledgements

This bachelor thesis was performed at the physics department at Lund University in collaboration with the Centre for Ocean and Ice at the Danish Meteorology Institute. All data used in this work were provided by the Danish Meteorology Institute.

First of all I would like to thank my supervisors Martin Nissen and Elna Nilsson Heimdal for all the advice and support during the preparation of this thesis. Special thanks to Gorm Dybkjær for many valuable suggestions and inspiration. Finally I wish to thank all the happy and friendly souls at the Centre for Ocean and Ice for their support and warm welcoming.

8. References

[1] S.Solomon, D.Qin, M.Manning, Z.Chen, M.Marquis, K.B.Averyt, M.Tignor and H.L.Miller, *The Physical Science Basis*, Contribution of Working Group I to the Fourth Assessment Report of the Intergovernmental Panel on Climate Change (IPCC), Cambridge University Press, Cambridge, United Kingdom and New York, NY, USA (2007)

[2] The Cryosphere Today, *Compare Daily Sea Ice*, Polar Research Group, University of Illinois at Urbana-Champaign, Department of Atmospheric Sciences (Electronic) http://arctic.atmos.uiuc.edu/cryosphere/ (2013-05-21)

[3] S.Stoyanova, NASA, *Arctic Sea Ice Continues to Decline, Arctic Temperatures Continue to Rise In 2005* (Electronic), last updated: 2008-02-23. http://www.nasa.gov/centers/goddard/news/topstory/2005/arcticice_decline.html (2013-05-16)

[4] J.Comiso, P.Wadhams, L.Toudal Pedersen and R. Gersten, *Seasonal and Interannual Variability of the Odden Ice Tongue and a Study of Environmental Effects*, Journal of Geophysical Research, vol.106, issue C5, p. 9093-9116 (2001)

[5] M.Brandt Jensen, *Arctic Sea Ice Variability and Trends 1979-2007*, Master Thesis (2011)

[6] H.Haak, J.Jungclaus, T.Koenigk and U.Mikolajewicz, *Variability of Fram Strait Sea Ice Export: Cause, Impacts and Feedbacks in a coupled climate model*, Climate Dynamics, vol.26, p.17-34 (2006)

[7] P.Wadhams, *Ice in the Ocean*, Gordon and Breach Science Publishers, University of Cambridge, UK (2000)

[8] S.Sandven, A.Sirevaag, L.Smedrud, A.Sorteberg and K.Kloster, *Recent Dind Driven High Sea Ice Area Export in the Fram Strait Contributes to Arctic Sea Ice Decline*, The Cryosphere, 5, p.821-829 (2011)

[9] J.Weiss, *Drift, Deformation and Fracture of Sea Ice*, Springer Briefs in Earth Sciences (2013)

[10] T.Vinje, *Fram Strait Ice Fluxes and Atmospheric Circulation: 1950-2000*, Journal of Climate, vol.14, p.3508-3517 (2000)

[11] M.Hilmer and T.Jung, *Evidence for a Recent Change in the Link Between the North Atlantic Oscillation and the Arctic Sea Ice Export*, Geophysical Research Letters, vol.27, No.7, p.989-992 (2000)

[12] R.Kwok, G.Cunningham and S.Pang, *Fram Strait Sea Ice Outflow*, Journal of Geophysical Research, vol.109, C01009 (2004)
[13] Personal Communication with Gorm Dybkjær, Ice Specialist at Centre for Ocean and Ice, Danish Metrology Institute (DMI) (2013-05-23)

[14] IBCAO, *The International Bathymetric Chart of the Arctic Ocean* (2008) (Electronic) http://www.ibcao.org

[15] L.T.Pedersen, R.T.Tonboe, M. Brandt Jensen, G.Dybkjær, M.Nissen, J.Rasmussen, S.M.Olsen, H.Skourup, R.Saldo and R.Forsberg, *KANUMAS MET/ICE/OCean Overview Report 2011 - East Greenland* (2011)

[16] Arctic Monitoring and Assessment Programme (AMAP), *Assessment Report: Arctic Pollution Issues* (1998)

[17] H.Eicken, *From the Microscopic, to the Macroscopic, to the Regional Scale: Growth, Microstructure and Properties of Sea Ice,* Sea ice, p.22-81 (2003)

[18] J.Cappelen, *Greenland - DMI Historical Climate Data Collection 1873-2012*, Technical Report 13-04 (2012)

[19] National Oceanic & Atmospheric Administration (NOAA), *Visualize CDC Derived NCEP Reanalysis Products Surface Level Data*, Earth System Research Laboratory, Physical Science Division (Electronic) http://www.esrl.noaa.gov/psd/cgi-bin/DataAccess.pl?DB_dataset=CDC+Derived+NCEP+Reanalysis+Products+Surface+Level&DB_variable=Sea+Level+Pressure&DB_statistic=Long+Term+Mean&DB_tid=30684&DB_did=39&DB_vid=2560 (2013-05-22)

[20] National Snow and Ice Data Centre (NSIDC), *All About Arctic Climatology and Meteorology*, (Electronic) http://nsidc.org/cryosphere/arctic-meteorology/index.html (2013-05-16)

[21] The Map Factory, *Arctic Oscillation* (Electronic) http://www.the-m-factory.com/portfolio/maps/trad_maps_07.html (2013-05-22)

[22] BA Education Powerpoint, Danish Meteorology Institute (DMI), *4-5: Havis leksikon* (2012)

[23] D.Lubin and R.Massom, *Polar Remote Sensing - Atmosphere and Oceans*, vol.1, Springer Praxis Publishing Ltd, Chichester, U.K (2006)

[24] Ideo, Columbia, *Why We Care: Sea-Ice Basics*, (Electronic) http://www.ldeo.columbia.edu/~louisab/sedpage/basics.html (2013-05-22)

[25] S.Sandven and O.M.Johannessen, *Sea Ice Monitoring by Remote Sensing*, Manual of Remote Sensing: Remote Sensing of the Marine Environment, 3rd Ed, vol.6, p.241-283 (2006)

[26] National Aeronautics and Space Administration (NASA), *Impacts of a Warming Arctic*, Global Climate Change (Electronic) http://climate.nasa.gov/education/pbs_modules/lesson2Engage (2013-05-22)

[27] National Snow and Ice Data Centre (NSIDC), *All About Sea Ice*, (Electronic) http://nsidc.org/cryosphere/seaice/index.html (2013-05-16)

[28] C.Haas, *Dynamics versus Thermodynamics: The Sea Ice Thickness Distribution*, Sea Ice, p.82-111 (2003)

[29] G.Dieckmann and H.Hellmer, *The Importance of Sea Ice: An Overview*, Sea Ice, p.1-21 (2003)

[30] National Snow and Ice Data Centre (NSIDC), *Satellite estimates show continued thinning*, Arctic Sea Ice News & Analysis, Monthly Archives April 2013 (Electronic) http://nsidc.org/arcticseaicenews/2013/04/ (2013-05-30)

[31] A.V.Bushuyev, WMO, *Sea Ice Nomenclature*, version 1.0 (Electronic) http://www.aari.nw.ru/gdsidb/docs/wmo/nomenclature/WMO_Nomenclature_draft_version1-0.pdf

[32] US Army Corps of Engineer, *Remote Sensing*, Engineer Manual (2003)

[33] I.A.Robinson, *Measuring the Oceans from Space*, Springer Praxis Publishing, Chichester, U.K (2004)

[34] Danish Meteorology Institute (DMI), *Ice Charts*, (Electronic) http://www.dmi.dk/dmi/en/gronland/iskort.htm (2013-05-21)

[35] Canadian Space Agency, *Satellite Characteristics*, (Electronic) last updated: 2011-01-21 http://www.asc-csa.gc.ca/eng/satellites/radarsat/radarsat-tableau.asp (2013-05-21)

[36] Personal Communication with Martin Nissen, Ice Specialist at Centre for Ocean and Ice, Danish Metrology Institute (DMI) (2013-05-23)

[37] European Space Agency (ESA), *Envisat Overview*, (Electronic) last updated: 2013-01-09 http://www.esa.int/Our_Activities/Observing_the_Earth/Envisat_overview (2013-05-21)

[38] National Aeronautics and Space Administration (NASA), *MODIS*, (Electronic) http://modis.gsfc.nasa.gov/about/ (2013-05-21)

[39] National Environmental Satellite, Data and Information Service (NOAA), *Advanced Very High Resolution Radiometer - AVHRR*, (Electronic) last updated: 2013-03-28 http://noaasis.noaa.gov/NOAASIS/ml/avhrr.html (2013-05-21)

[40] World Metrology Organization (WMO), *Ice Chart Colour Code Standard*, JCOMM Technical Report, No. 24 (2004)

[41] K.Qvistgaard and H.Valeur, *Iscentralen 50 år - i glimt* (2009)

[42] Remote Sensing Systems, *Description of SSM/I & SSMIS Data Products*, (Electronic) last updated: 2012-09-05 http://www.ssmi.com/ssmi/ssmi_description.html (2013-05-21)

[43] Ocean and Sea Ice SAF (OSISAF), *Sea Ice Products*, (Electronic)
last updated: 2013-05-30
http://osisaf.met.no/p/ice/index.html (2013-05-22)

[44] L.Breivik, T.Carriers, S.Eastwood, A.Fleming, F.Girard-Ardhuin, J.Karvonen, R.Kwok, W.Meier, M.Mäkynen, L.Toudal Pedersen, S.Sandven, M.Similä and R.Tonboe, *Remote Sensing of Sea Ice*, Proceedings of OceanObs'09: Sustained Ocean Observations and Information for Society, vol. 2. (2010)